Intersections of Lamb Mode Dispersion Curves for an Isotropic Plate

by

Madiha Kausar Jabeen

A thesis submitted in partial fulllment of the requirements
for the degree of Master of science in Mathematics

Supervised by

Prof. Faiz Ahmad
School of Natural Sciences
National University of Sciences and Technology
Islamabad, Pakistan

National University of Sciences & Technology

MASTER'S THESIS WORK

We hereby recommend that the dissertation prepared under our supervision by: Ms. Madiha Kausar Jabeen, Regn No. 00000117015 Titled: Intersections of the Lamb Mode Dispersion Curves of an Isotropic Plate be accepted in partial fulfillment of the requirements for the award of **MS** degree.

Examination Committee Members

1. Name: Dr. Moniba Shams   Signature: _____

2. Name: Dr. Mujeeb ur Rehman   Signature: _____

3. Name: _____   Signature: _____

4. Name: Dr. Nabeela Kausar   Signature: _____

Supervisor's Name: Prof. Faiz Ahmad   Signature: _____

_____   29-08-2017

Head of Department   Date

COUNTERSINGED

Date: 29/8/17   **Dean/Principal**

THESIS ACCEPTANCE CERTIFICATE

Certified that final copy of MS thesis written by **Ms. Madiha Kausar Jabeen,** (Registration No. **00000117015**), of **School of Natural Sciences** has been vetted by undersigned, found complete in all respects as per NUST statutes/regulations, is free of plagiarism, errors, and mistakes and is accepted as partial fulfillment for award of MS/M.Phil degree. It is further certified that necessary amendments as pointed out by GEC members and external examiner of the scholar have also been incorporated in the said thesis.

Signature: _Faiz Ahmad_

Name of Supervisor Prof. Faiz Ahmad

Date: _29. 08. 17_

Signature (HoD): _____

Date: _29 - 08 - 2017_

Signature (Dean/Principal): _____

Date: _29/8/17_

Abstract

In this thesis we discuss the points of intersection of the symmetric and antisymmetric Lamb mode dispersion curves of an isotropic plate. The Rayleigh-Lamb frequency relation for dispersion curves is derived for a plate with thickness 2h and their intersections are determined. The points of intersection are graphically represented.

The plateau region possessed by the Lamb modes in k-c plane is graphically shown for an isotropic plate where k is the wave number and c is the wave speed. Lastly, the reflection of SV-waves is mathematically examined and the mode conversion through this reflection is discussed analytically. An expression is derived which gives the bound in which mode conversion can take place and outside which it is forbidden.

Acknowledgement

First and foremost, I am thankful to Almighty Allah the most Gracious and Merciful, Who gives power to the weak and helps the helpless.

I would like to express my gratitude to my supervisor, Professor Faiz Ahmad, for directing me throughout this research. I will always be thankful for the learning opportunities he has provided, for his kindness and patience.

I want to thank my parents, who have made enormous efforts to make it possible. Thank you so much for believing in me, for your support, endless love and prayers.

At the end, I would also like to thank my family and friends, for their help and encouragement. I wish them all the health and success in life.

Madiha Kausar Jabeen

To My Loving Parents

Contents

Chapter 1

Introduction

A waveguide allows a wave to propagate through a mechanical structure (like a plate or a rod). Radio waves, electromagnetic waves, acoustic waves etc are its examples. The guided wave, propagating along the stress free boundary of an elastic half space is called Rayleigh wave. A single layered half space can be a waveguide for Love waves while Lamb wave is the guided wave that propagates in a plate.

Guided waves help widely in non-destructive testing (NDT) which is a strategy used to describe the material properties like its thickness, interior structure and out of sight imperfections without giving any harm to it. In this technique, waves are sent into the material being tested and they propagate through it by vibrating the particles that make up the material. The reflected waves give information about the deformities present in the sample.

In 1885 Lord Rayleigh [1] predicted the presence of waves along the surface of solids. These were named after him as Rayleigh waves. Moreover, when these waves propagate through a layer then these are named as Rayleigh-Lamb or Lamb waves. Lamb [2] in 1917 presented frequency relation for a wave propagating in a plate known as Rayleigh-Lamb dispersion relation. A comprehensive theory for such waves was presented by Mindlin [3] in 1950. A test confirmation of the utilization of Lamb waves in NDT was given by Worlton [4] in 1961.

Lamb waves are guided waves that propagate in the solid plates having symmetric and antisymmetric modes. As the Lamb waves depend upon frequency of a wave, so the number of modes increases with the increasing frequency which

gives rise to infinite number of symmetric and antisymmetric modes. Generally Lamb modes can be used for material characterization and to identify the defects present in it. It is also used for pipeline and composites inspection. Propagation of Lamb waves depend on the properties of material like its thickness, density etc.

Graphically, symmetric and antisymmetric Lamb mode dispersion curves appear to intersect each other at some points. Freedman [5] explained the occurrence of intersection of lamb modes and its variation with Poisson ratio on it's full allowed range using Mindlin's method of bounds [3]. In 2016, A. G. Every [6] classified these intersections into three types, Type F, Type I, Type II and examined these intersections for some materials.

Plane waves can be allowed to coincide at the interface in a medium made up of two half spaces with different material properties. Suppose a plane wave is incident upon a plane surface that is an interface between two materials. The incident wave originates in one medium but for the stresses and displacements of a propagating wave to be continuous at interface the additional reflected and refracted waves are required. J. D. Achenbach [9] determined the reflection of various plane harmonic waves like P-wave, S-wave, SV-wave and SH-wave in joined half space.

Plan of dissertation

This thesis concerns with the study of Lamb modes dispersion curves and their intersections. In the present chapter the introduction is given.

Chapter 2 comprises of some basic definitions of terms used in the thesis.

Chapter 3 takes into account the investigation of Lamb modes in an isotropic plate in detail, Rayleigh-Lamb dispersion relation for symmetric and antisymmetric modes is presented by using the Helmholtz decomposition of the displacement vector and is also graphically represented.

Chapter 4 describes, in some detail, work of Every [6] dealing with the points of intersection of symmetric and antisymmetric Lamb modes for an isotropic plate. The graphical representation is given in this chapter to show intersection points. Also the study of the plateau region shown by Lamb mode dispersion curves is graphically represented.

Chapter 5 deals with the study of reflection of SV-waves and the solution set is calculated for reflected SV-waves. It also deals with the study of mode conversion due to reflection of an SV-wave from the surface of a half space. An analytical expression is derived to get a range in which mode conversion can take place.

Chapter 2

Preliminaries

Wave

A wave can be portrayed as a disturbance that goes through a medium from one point to another. Waves are surrounding us like the sound waves, light waves and the most obvious example is the ripples created on water surface by a stone thrown into it.

Each type of wave exhibits a particular characteristic that is used to recognize it. The two main types of wave are given below:

2.1 Body waves

The waves that can travel through an infinite medium are termed as body waves. They are further categorized into two types:

• **Longitudinal waves** - They are also named as P-waves or primary waves. Displacement of particles is parallel to the direction of propagation of wave in this case. Sound waves moving through the air is an example of this type of wave.

• **Transverse waves** - They are also named as S-waves or secondary wave. In this case, the displacement of particles is perpendicular to the direction of propagation of wave. Movement of a wave through a solid object like a stretched rope is an example of this type of wave.

2.2 Surface waves

Unlike the body waves these waves can only move along the surface and occur at interfaces with circular motion of particles. Waves in the ocean and ripples on the surface of water are its examples. In an earthquake, these waves can cause the most damage. These waves are also categorized into two types:

• **Love waves** - Love waves are named after Augustus Edward Hugh Love who discovered them in a thin layer over a half space and found that the particles in these waves do not move in a rotating mode rather, similar to S-waves, these waves move forward and backward perpendicular to the direction of wave propagation.

• **Rayleigh waves** - Rayleigh waves were named after Lord Rayleigh, these waves are a blend of transverse and longitudinal waves. The particle movement in these waves seems similar to the surface waves but observing deliberately, one will see that the motion of particles is not the same. In surface waves, every molecule makes a round movement perpendicular to the direction of propagation of wave like water waves. While in Rayleigh waves, the particles make an elliptical movement against the direction of propagation of wave.

Rayleigh waves when propagate through the layer of a solid plate then are termed as *Lamb waves*. Lamb waves with infinite set of symmetric and antisymmetric modes can be produced in a plate with free edges.

Isotropic Material

A material, the properties of which do not depend on the direction is said to be an isotropic material. Glass and metals like steel, ceramics are examples of isotropic materials.

Hooke's Law for an isotropic material given by [9] is:

$$T_{ij} = \lambda S_{kk}\delta_{ij} + 2\mu S_{ij}.$$

where T_{ij} and S_{ij} are components of stress tensor and strain tensor respectively and λ, μ are Lame constants.

Auxetic material

If we consider an isotropic elastic material, then the elastic response of the material is described fully by four inter-related properties: Poisson's ratio, Young's modulus, shear modulus and bulk modulus. The range of Poisson's ratio for isotropic materials is between -1 and +0.5.

From the relationship between shear modulus, bulk modulus and Poisson's ratio it turns out that the positive limit for Poisson's ratio (corresponding to rubber) provides a material that is easy to deform (through shearing) but is relatively incompressible. On the other hand, the negative limit for Poisson's ratio of -1 produces a material that is difficult to shear (i.e. it maintains shape) but is relatively compressible (changes volume easily).

Auxetic materials are the one that exhibit negative Poisson's ratio. They are used in many sports items like pads, gloves, helmets, footwear soles etc.

Incident, reflected and refracted waves

An incident wave originates from a source of wave production in a medium. Reflection means that the wave is turned back into the half-space from which it came, while a change in the direction of waves as they pass from one medium to another is called refraction of waves.

Mode conversion

In mode conversion one type of wave can be changed into another type. Mode conversion occurs when a wave is reflected from a surface or it encounters an interface between materials of different acoustic impedances and the incidence is not normal to the interface. For example, when a primary wave hits an interface with an angle then some of the energy can cause particle movement in the transverse direction to start a secondary wave.

Chapter 3

Lamb modes in a plate

Lamb waves were named after the mathematician Horace Lamb in 1917, who discovered them in solid plates that allows two infinite sets of Lamb wave modes to propagate with velocities depending upon the relationship between wavelength and thickness of the plate. These are the guided waves that can be used to inspect the material properties.

This chapter includes the study of Rayleigh-Lamb frequency relation for an isotropic plate using Helmholtz decomposition of displacement vector into scalar and vector potential. The graphical representation of Lamb modes for some materials is also included.

3.1   Introduction

In this chapter, we follow the theory presented by Achenbach [9]. In Helmholtz decomposition, a vector function $\boldsymbol{v} \in C^2$ can be decomposed into a sum of two vectors given by [9]

$$\boldsymbol{v} = \boldsymbol{v_1} + \boldsymbol{v_2},$$

such that

$$\boldsymbol{v_1} = \nabla \phi,$$

$$\boldsymbol{v_2} = \nabla \times \boldsymbol{\psi},$$

$$\Rightarrow \boldsymbol{v} = \nabla \phi + \nabla \times \boldsymbol{\psi}. \tag{3.1.1}$$

where ϕ is called the scalar potential and $\boldsymbol{\psi}$ is called the vector potential.
The equation of motion for displacement $\boldsymbol{v}$ is given below:

$$\mu\nabla^2\boldsymbol{v} + (\lambda + \mu)\nabla(\nabla.\boldsymbol{v}) = \rho\ddot{\boldsymbol{v}}. \tag{3.1.2}$$

Using Eq (3.1.1) in (3.1.2), we have

$$\mu\nabla^2(\nabla\phi + \nabla \times \boldsymbol{\psi}) + (\lambda + \mu)\nabla(\nabla.(\nabla\phi, +\nabla \times \boldsymbol{\psi})) = \rho(\nabla\ddot{\phi} + \nabla \times \ddot{\boldsymbol{\psi}}),$$

$$\mu\nabla^2\nabla\phi + \mu\nabla^2\nabla \times \boldsymbol{\psi} + (\lambda + \mu)(\nabla.\nabla^2\phi + \nabla.\nabla \times \boldsymbol{\psi}) = \rho(\nabla\ddot{\phi} + \nabla \times \ddot{\boldsymbol{\psi}}),$$

as we know that $\nabla^2\nabla\phi = \nabla\nabla^2\phi$ and $\nabla.\nabla \times \boldsymbol{\psi} = 0$. Using these relations in equation above, we get

$$\mu\nabla^2\nabla\phi + \mu\nabla^2\nabla \times \boldsymbol{\psi} + \lambda\nabla\nabla^2\phi + \mu\nabla\nabla^2\phi = \rho(\nabla\ddot{\phi} + \nabla \times \ddot{\boldsymbol{\psi}}),$$

$$\mu\nabla^2\nabla\phi + \mu\nabla^2\nabla \times \boldsymbol{\psi} + \lambda\nabla\nabla^2\phi + \mu\nabla\nabla^2\phi - \rho\nabla\ddot{\phi} - \rho\nabla \times \ddot{\boldsymbol{\psi}} = 0,$$

$$\nabla((\lambda + 2\mu)\nabla^2\phi - \rho\ddot{\phi}) + \nabla \times (\mu\nabla^2\boldsymbol{\psi} - \rho\ddot{\boldsymbol{\psi}}) = 0.$$

where ϕ and $\boldsymbol{\psi}$ are some potential functions.
If we choose ϕ such that

$$(\lambda + 2\mu)\nabla^2\phi - \rho\ddot{\phi} = 0,$$

$$\Rightarrow \nabla^2\phi - \frac{1}{c_L^2}\ddot{\phi} = 0.$$

and $\boldsymbol{\psi}$ such that

$$\nabla \times (\mu\nabla^2\boldsymbol{\psi} - \rho\ddot{\boldsymbol{\psi}}) = 0,$$

$$\Rightarrow \nabla^2\boldsymbol{\psi} - \frac{1}{c_T^2}\ddot{\boldsymbol{\psi}} = 0,$$

then Eq (3.1.1) will be the solution of Eq (3.1.2).
Here, c_L and c_T are speeds of longitudinal and transverse waves respectively with
$c_L{}^2 = \frac{\lambda+2\mu}{\rho}$ and $c_T{}^2 = \frac{\mu}{\rho}$.

3.2   Dispersion relation for Lamb modes

Consider a wave propagating through a plate with thickness 2h. In a plane strain independent of x_3-axis, the vector is of the form [9]

$$\boldsymbol{v}(x_1, x_2, t) = v_1(x_1, x_2, t)\boldsymbol{i} + v_2(x_1, x_2, t)\boldsymbol{j} \quad and \quad v_3 = 0.$$

8

$$\nabla \times \boldsymbol{\psi} = \boldsymbol{i}(\frac{\partial \psi_3}{\partial x_2} - \frac{\partial \psi_2}{\partial x_3}) - \boldsymbol{j}(\frac{\partial \psi_3}{\partial x_1} - \frac{\partial \psi_1}{\partial x_3}) + \boldsymbol{k}(\frac{\partial \psi_2}{\partial x_2} - \frac{\partial \psi_1}{\partial x_2}),$$

Since the considered motion is in the $x_1 x_2$-plane so ψ_1 and ψ_2 are independent of x_3-axis which made them zero, so we are left with

$$\nabla \times \boldsymbol{\psi} = \boldsymbol{i}(\frac{\partial \psi_3}{\partial x_2}) - \boldsymbol{j}(\frac{\partial \psi_3}{\partial x_1}).$$

The Helmholtz displacement components given by Achenbach [9] are of the form

$$v_1 = \frac{\partial \phi}{\partial x_1} + \frac{\partial \psi_3}{\partial x_2}, \tag{3.2.1}$$

$$v_2 = \frac{\partial \phi}{\partial x_2} - \frac{\partial \psi_3}{\partial x_1}. \tag{3.2.2}$$

Using a common form of Hooke's law for isotropic materials to calculate stress, we have

$$\tau_{11} = 2\mu \frac{\partial v_1}{\partial x_1} + \lambda(\frac{\partial v_1}{\partial x_1} + \frac{\partial v_2}{\partial x_2}), \tag{3.2.3}$$

$$\tau_{12} = \mu(\frac{\partial v_2}{\partial x_1} + \frac{\partial v_1}{\partial x_2}), \tag{3.2.4}$$

$$\tau_{22} = 2\mu \frac{\partial v_2}{\partial x_2} + \lambda(\frac{\partial v_1}{\partial x_1} + \frac{\partial v_2}{\partial x_2}). \tag{3.2.5}$$

Now by using Eq (3.2.1) and (3.2.2) in Eq (3.2.3) − (3.2.5), the stress strain relation becomes

$$\tau_{11} = 2\mu(\frac{\partial^2 \phi}{\partial x_1^2} + \frac{\partial^2 \psi_3}{\partial x_1 \partial x_2}) + \lambda(\frac{\partial^2 \phi}{\partial x_1^2} + \frac{\partial^2 \phi}{\partial x_2^2}), \tag{3.2.6}$$

$$\tau_{12} = \mu(\frac{\partial^2 \psi_3}{\partial x_2^2} - \frac{\partial^2 \psi_3}{\partial x_1^2} + 2\frac{\partial^2 \phi}{\partial x_1 \partial x_2}), \tag{3.2.7}$$

$$\tau_{22} = 2\mu(\frac{\partial^2 \phi}{\partial x_2^2} - \frac{\partial^2 \psi_3}{\partial x_1 \partial x_2}) + \lambda(\frac{\partial^2 \phi}{\partial x_1^2} + \frac{\partial^2 \phi}{\partial x_2^2}). \tag{3.2.8}$$

with ϕ and ψ_3 satisfying the following equations

$$\nabla^2 \phi = \frac{1}{c_L^2} \ddot{\phi}. \tag{3.2.9}$$

$$\nabla^2 \psi_3 = \frac{1}{c_T^2} \ddot{\psi}_3. \tag{3.2.10}$$

Let the solution of wave condition is given by the following form

$$\phi(x_1, x_2) = \Phi(x_2) \exp[ik(x_1 - ct)]. \tag{3.2.11}$$

$$\boldsymbol{\psi}(x_1, x_2) = \Psi(x_2) \exp[ik(x_1 - ct)]. \tag{3.2.12}$$

9

Where c and k represents the speed and the wave number of a wave respectively. From Eq (3.2.9) and (3.2.11), we have

$$-k^2\Phi + \Phi'' = -(\frac{k^2c^2}{c_L^2})\Phi,$$

$$\Phi'' + p^2\Phi = 0. \tag{3.2.13}$$

where $\Phi'' = \frac{d^2\Phi}{dx_2^2}$ and $p^2 = (\frac{c^2}{c_L^2} - 1)k^2$.

Similarly from Eq (3.2.10) and (3.2.12)

$$-k^2\Psi + \Psi'' = -(\frac{k^2c^2}{c_T^2})\Psi,$$

$$\Psi'' + q^2\Psi = 0. \tag{3.2.14}$$

where $\Psi'' = \frac{d^2\Psi}{dx_2^2}$ and $q^2 = (\frac{c^2}{c_T^2} - 1)k^2$.

The solution of Eq (3.2.13) and (3.2.14) is given by

$$\Phi(x_2) = A_1\sin(px_2) + A_2\cos(px_2),$$

$$\Psi(x_2) = B_1\sin(qx_2) + B_2\cos(qx_2).$$

Using above relations in Eq $(3.2.1), (3.2.2), (3.2.6) - (3.2.8), (3.2.11)$ and $(3.2.12)$ and ignoring the exponential term in the continuation since it shows up in every one of the expressions and does not takes part in calculating frequency relation, we have

$$\phi = A_1\sin(px_2) + A_2\cos(px_2),$$

$$\psi_3 = B_1\sin(qx_2) + B_2\cos(qx_2),$$

$$v_1 = ik[A_1\sin(px_2) + A_2\cos(px_2)] + q[B_1\cos(qx_2) - B_2\sin(qx_2)],$$

$$v_2 = p[A_1\cos(px_2) - A_2\sin(px_2)] - ik[B_1\sin(qx_2) + B_2\cos(qx_2)],$$

$$\tau_{12} = \mu[2ikp(A_1\cos(px_2) - A_2\sin(px_2)) + (k^2 - q^2)(B_1\sin(qx_2) + B_2\cos(qx_2))],$$

$$\tau_{11} = 2\mu[-k^2(A_1\sin(px_2) + A_2\cos(px_2)) - ikq(B_1\cos(qx_2) + B_2\sin(qx_2))]$$
$$-\lambda[(k^2 + p^2)(A_1\sin(px_2) + A_2\cos(px_2))],$$

$$\tau_{22} = -2\mu[p^2(A_1\sin(px_2) + A_2\cos(px_2)) + ikq(B_1\cos(qx_2) - B_2\sin(qx_2))]$$
$$-\lambda[(k^2 + p^2)(A_1\sin(px_2) + A_2\cos(px_2))].$$

To calculate the frequency relation we split the wave passing through the plate into symmetric and antisymmetric modes. If the expression for v_1 have cosines

10

(sines) then $x_2 = 0$ and the motion of wave in x_1-direction will be symmetric (antisymmetric), while if the expression for v_2 have sines (cosines) then the motion of wave in x_2-direction will be symmetric (antisymmetric).

For a symmetric mode problem we consider the following equations:

$$\Phi = A_2 \cos(px_2),$$

$$\Psi = B_1 \sin(qx_2),$$

$$v_1 = ikA_2 \cos(px_2) + qB_1 \cos(qx_2),$$

$$v_2 = -ikB_1 \sin(qx_2) - pA_2 \sin(qx_2),$$

$$\tau_{12} = -2ikp\mu A_2 \sin(px_2) + \mu(k^2 - q^2)B_1 \sin(qx_2),$$

$$\tau_{22} = -\lambda(k^2 + p^2)A_2 \cos(px_2) - 2\mu[p^2 A_2 \cos(px_2) + ikq(B_1 \cos(qx_2))].$$

Similarly for antisymmetric mode problem we consider the following equations:

$$\Phi = A_1 \sin(px_2),$$

$$\Psi = B_2 \cos(qx_2),$$

$$v_1 = ikA_1 \sin(px_2) - qB_2 \sin(qx_2),$$

$$v_2 = -ikB_2 \cos(qx_2) + pA_1 \cos(px_2),$$

$$\tau_{12} = 2ikp\mu A_1 \cos(px_2) + \mu(k^2 - q^2)B_2 \cos(qx_2),$$

$$\tau_{22} = -\lambda(k^2 + p^2)A_1 \sin(px_2) - 2\mu[p^2 A_1 \sin(px_2) - ikq(B_2 \sin(qx_2))].$$

On the free boundary of the plate having thickness 2h, we will use the following boundary conditions to get frequency relation:

$$at \quad x_2 = \pm h, \quad \tau_{21} = \tau_{22} = 0$$

For the symmetric modes, we have

$$\tau_{21} = [-2ikp \sin(px_2)A_2 + (k^2 - q^2) \sin(qx_2)B_1], \tag{3.2.15}$$

$$\tau_{22} = [(-k^2\lambda - p^2\lambda - 2\mu p^2) \cos(px_2)A_2 - 2ik\mu qB_1 \cos(qx_2)]. \tag{3.2.16}$$

As there are four boundary conditions for $x_2 = \pm h$, which will remain two because we will get the same equations for τ_{21}, similar remarks hold for τ_{22}.

Equation (3.2.15) from the boundary condition $\tau_{21} = 0$ and $x_2 = \pm h$ for all x_2, t becomes

$$-2ikp \sin(ph)A_2 + (k^2 - q^2) \sin(qh)B_1 = 0. \tag{3.2.17}$$

Equation (3.2.16) from the boundary condition $\tau_{22} = 0$ and $x_2 = \pm h$ for all x_2, t becomes

$$(-k^2\lambda - p^2\lambda - 2\mu p^2)\cos(ph)A_2 - 2ik\mu q\cos(qh)B_1 = 0. \tag{3.2.18}$$

As the equations (3.2.17) and (3.2.18) are homogeneous so their determinant must be zero, given by

$$-4k^2\mu pq\sin(ph)\cos(qh) + (k^2 - q^2)(\lambda k^2 + (\lambda + 2\mu)p^2)\sin(qh)\cos(ph) = 0,$$

In a more simplified form, we have

$$\frac{-4k^2\mu pq}{(k^2 - q^2)(\lambda k^2 + (\lambda + 2\mu)p^2)} + \frac{\tan(qh)}{\tan(ph)} = 0,$$

$$\frac{\tan(qh)}{\tan(ph)} = \frac{4k^2\mu pq}{(k^2 - q^2)(\lambda k^2 + (\lambda + 2\mu)p^2)}.$$

Further simplification leads to

$$\frac{\tan(qh)}{\tan(ph)} = -\frac{4k^2 pq}{(k^2 - q^2)^2}. \tag{3.2.19}$$

Equation (3.2.19) is the Rayleigh-Lamb frequency relation for symmetric modes. Now to find out the dispersion relation for antisymmetric modes we will use the boundary conditions and get the following set of equations

$$2ikp\cos(ph)A_1 + (k^2 - q^2)\cos(qh)B_2 = 0, \tag{3.2.20}$$

$$(-k^2\lambda - p^2\lambda - 2\mu p^2)\sin(ph)A_1 + 2ik\mu q\sin(qh)B_2 = 0, \tag{3.2.21}$$

Due to homogeneity, the determinant of equations above must be zero, so it yields

$$-4k^2\mu pq\tan(qh) + (k^2 - q^2)(\lambda k^2 + (\lambda + 2\mu)p^2)\tan(ph) = 0,$$

In more simplified form we have

$$\frac{-4k^2\mu pq}{(k^2 - q^2)(\lambda k^2 + (\lambda + 2\mu)p^2)} + \frac{\tan(ph)}{\tan(qh)} = 0,$$

$$\frac{\tan(ph)}{\tan(qh)} = \frac{4k^2\mu pq}{(k^2 - q^2)(\lambda k^2 + (\lambda + 2\mu)p^2)},$$

Further simplification finally yields

$$\frac{\tan(ph)}{\tan(qh)} = -\frac{4k^2 pq}{(k^2 - q^2)^2}. \tag{3.2.22}$$

Equation (3.2.22) is the Rayleigh-Lamb frequency relation for antisymmetric modes.

The spectrum of the symmetric Lamb modes has the following distinctive features:

• There exists no mode with phase speed less than c_R.

• There is only one mode whose speed asymptotically approaches c_R.

• A horizontal line above c=c_T (including the line c=c_L) cannot be an asymptote to any of the modes.

• Phase speed of all modes, except the lowest mode, approaches c_T as the frequency becomes very large.

Ahmad [10] analyzed the dispersion relation to understand the above features of the spectrum.

The figure (3.1) shows the graphical representation of the given features:
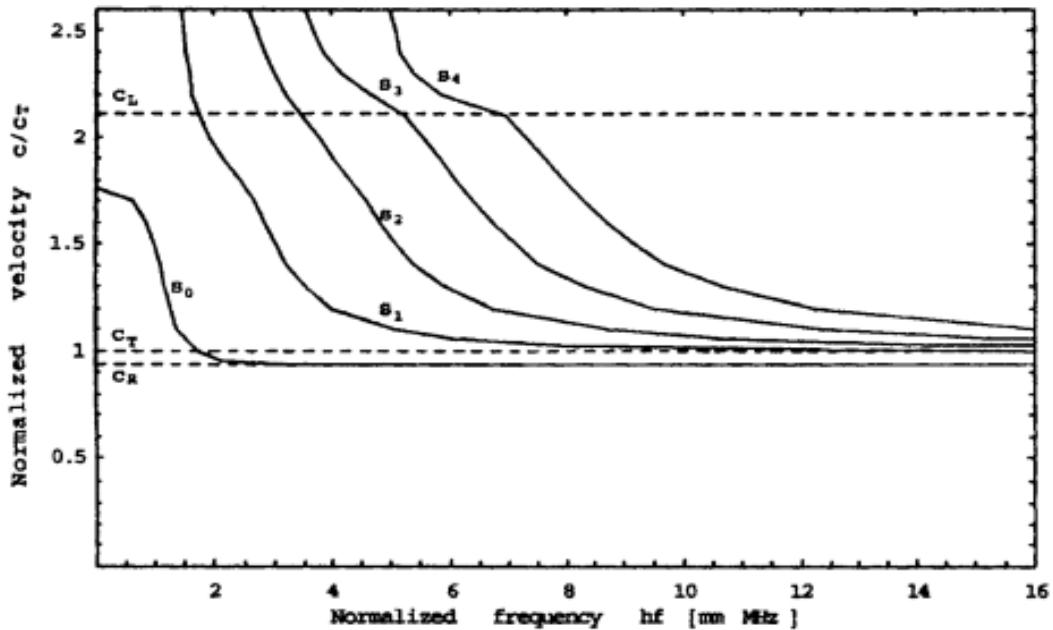
Figure 3.1: First five symmetric Lamb modes for aluminum plate.

He also found a simple formula for Lamb modes in a plate [11], this approximation holds for almost every mode when the phase velocity is in between c_T and c_L. Also, Ahmad [12] found an approximate expression for the longitudinal modes in a cylinder.

The figures (3.2) and (3.3) will show the symmetric and antisymmetric modes for an aluminum plate with $e = \frac{c_L}{c_T} = 2.0288$, where c_L and c_T are speeds of longitudinal and transverse waves respectively.
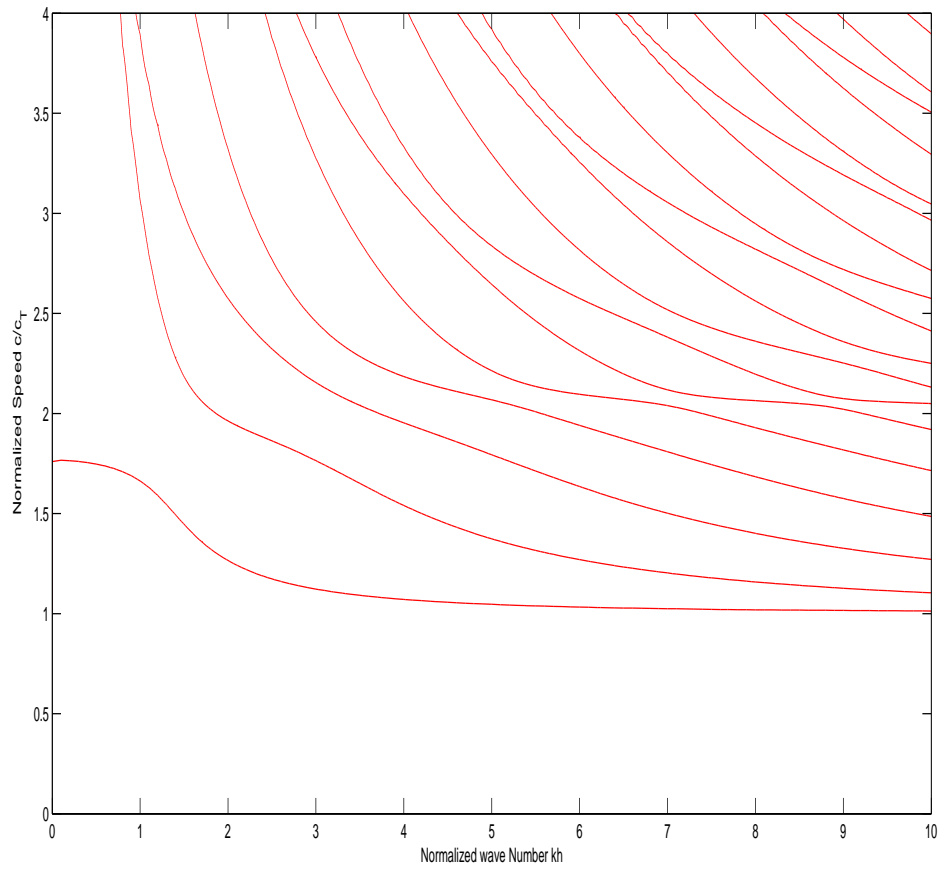

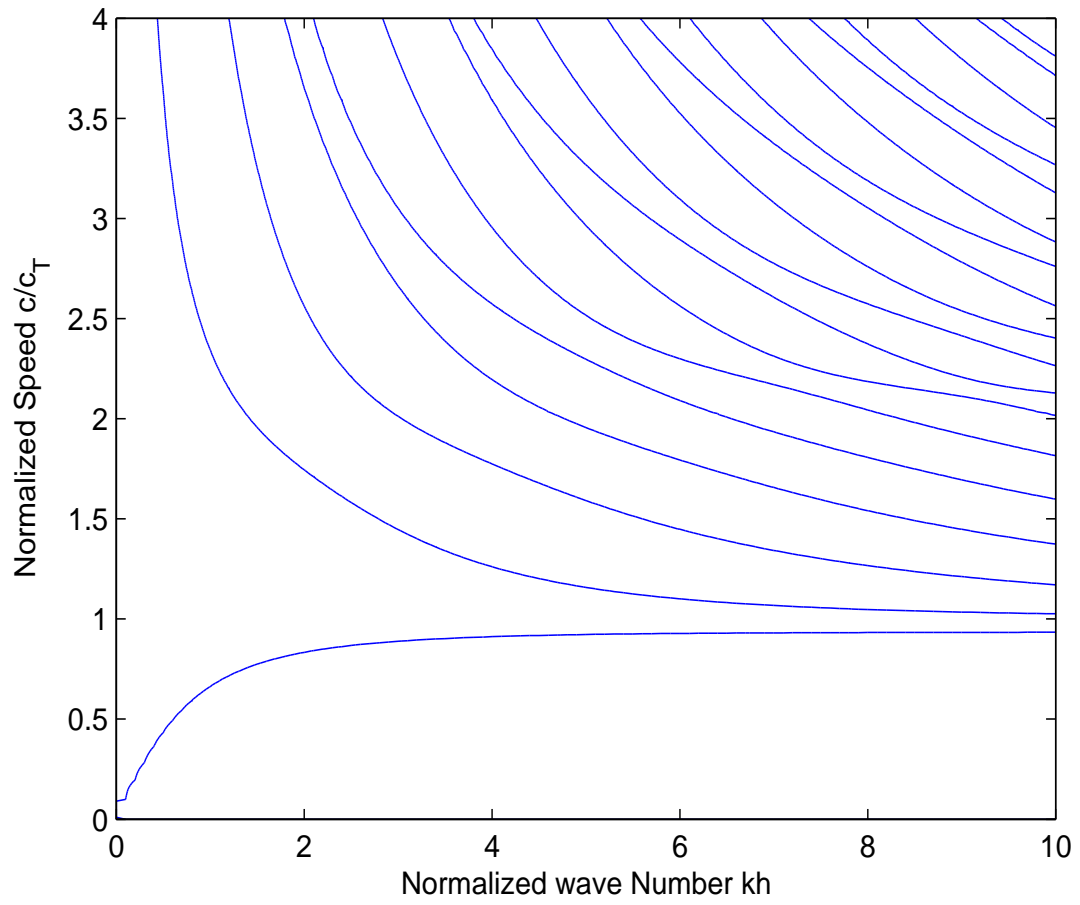Figure 3.2: Symmetric Lamb modes for an aluminum plate with $e = 2.0288$.

Figure 3.3: Antisymmetric Lamb modes for an aluminum plate with $e = 2.0288$.

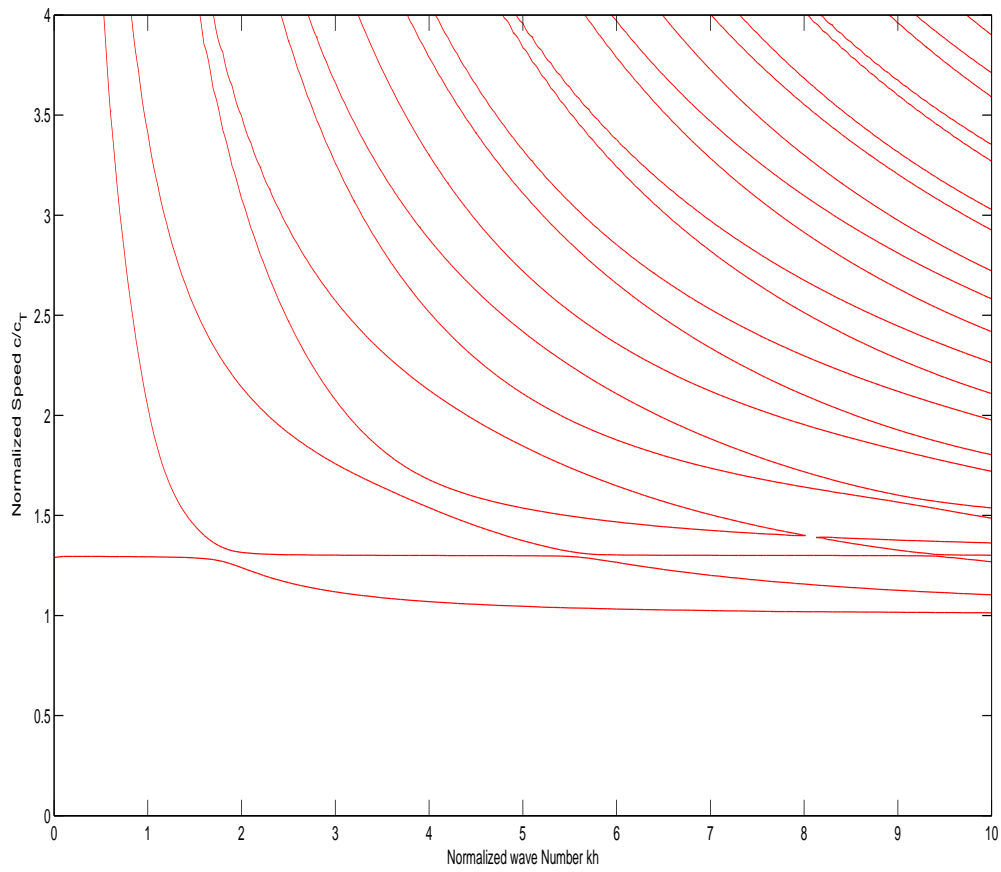The figures (3.4) and (3.5) will show the symmetric and antisymmetric modes for an auxetic material:

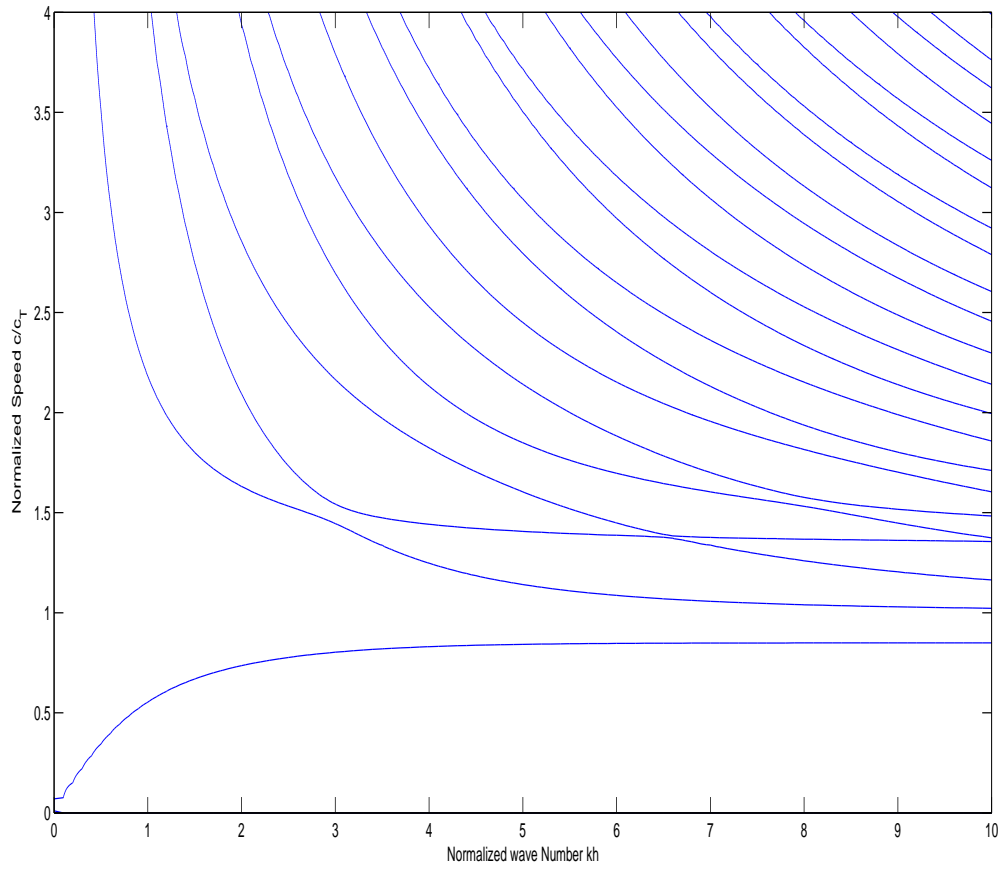Figure 3.4: Symmetric Lamb modes for an auxetic material with $e = 1.3$.

Figure 3.5: Antisymmetric Lamb modes for an auxetic material with $e = 1.3$.

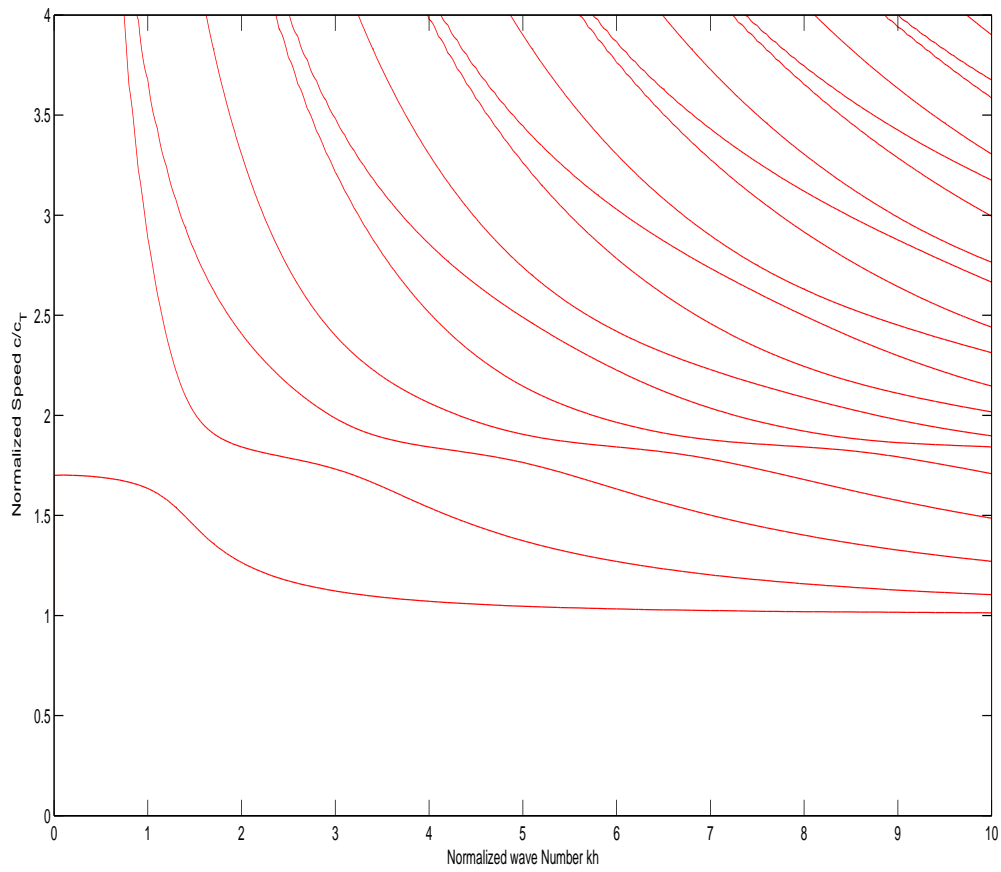The figures (3.6) and (3.7) will show the symmetric and antisymmetric modes for steel:

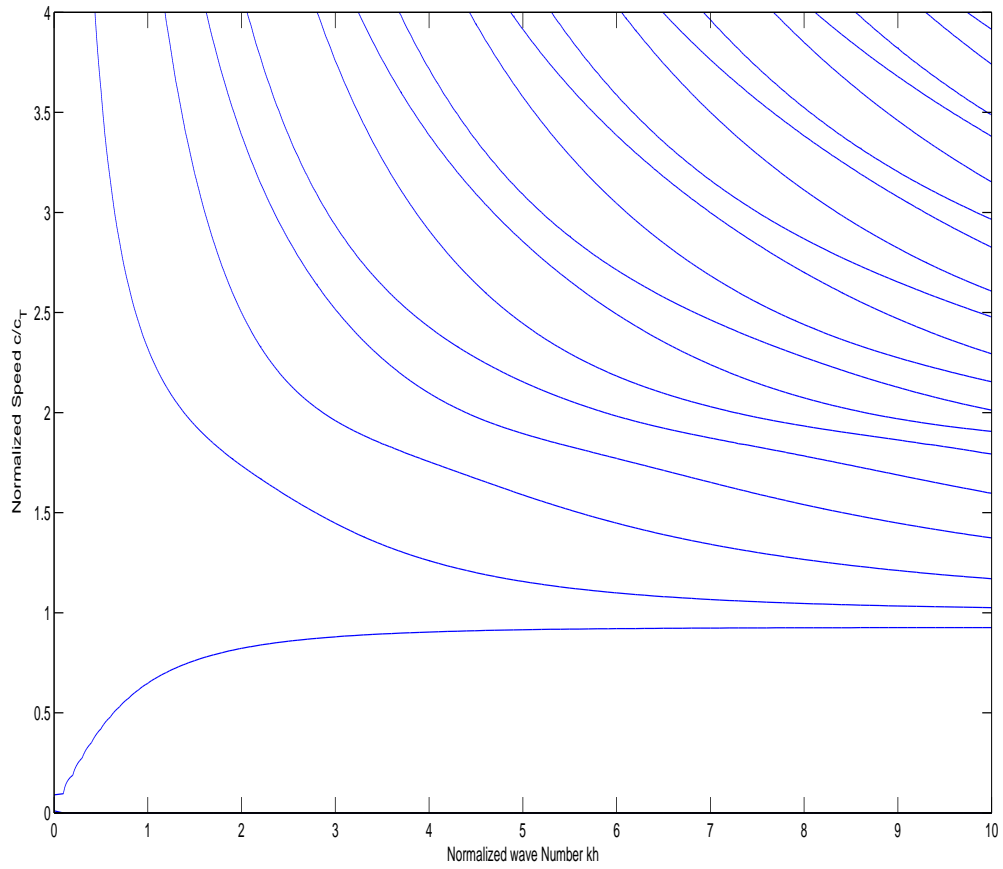Figure 3.6: Symmetric Lamb modes for steel with $e = 1.83$.

Figure 3.7: Antisymmetric Lamb modes for steel with $e = 1.83$.

Chapter 4

Intersections of the Lamb mode dispersion curves

The symmetric and antisymmetric Lamb modes when separately presented graphically, a family of curves is obtained, none of which crosses the other. On the other hand, when both the modes are plotted together then there exist some points in the graph where symmetric and antisymmetric curves appear to cross each other. These intersections between Lamb mode dispersion curves contribute widely in the study of the elastodynamics of free isotropic elastic plates.

The given chapter includes the different types of intersections of Lamb mode dispersion curves of stress free isotropic plate given by Every [6]. This work done is related to a search for supersonic surface acoustic waves on coated solids. These SSAWs possess a certain property which in some cases can be traced to intersections between the dispersion curves of the coat before it is applied on the material [7] [8]. The intersection of Lamb modes for different materials using k-c coordinates are graphically represented using MATLAB code. Also the appearance of plateau region in the graph when normalized speed is plotted against normalized wave number is graphically represented.

4.1 Introduction

The Rayleigh-Lamb frequency relation for symmetric and antisymmetric Lamb modes can also take the form

$$\frac{\tan(\frac{\pi}{2}\sqrt{\Omega^2 - \kappa^2})}{\tan(\frac{\pi}{2}\sqrt{\frac{\Omega^2}{e^2} - \kappa^2})} + F^{\pm 1}(\Omega, \kappa) = 0, \tag{4.1.1}$$

where

$$F^{+1}(\Omega, \kappa) = \frac{4\kappa^2 \sqrt{(\Omega^2 - \kappa^2)(\frac{\Omega^2}{e^2} - \kappa^2)}}{(\Omega^2 - 2\kappa^2)^2},$$

and

$$F^{-1}(\Omega, \kappa) = \frac{(\Omega^2 - 2\kappa^2)^2}{4\kappa^2 \sqrt{(\Omega^2 - \kappa^2)(\frac{\Omega^2}{e^2} - \kappa^2)}}.$$

The exponent of $F(\Omega, \kappa)$ is +1 for the symmetric modes and –1 for the antisymmetric modes.

The dimensionless frequency and dimensionless wave number in (4.1.1) is given by

$$\Omega = \frac{2\omega h}{\pi c_T}; \kappa = \frac{2kh}{\pi} \tag{4.1.2}$$

where ω is the angular frequency, h is the half thickness of the plate and k is the wave number.

Also

$$e = \frac{c_L}{c_T} = \sqrt{\frac{2(1-\sigma)}{(1-2\sigma)}}, \tag{4.1.3}$$

where c_L and c_T are the longitudinal and shear wave velocities, respectively. As the range for Poisson's ratio σ is $-1 < \sigma < 0.5$, so from the equation (4.1.3) e must be between $\sqrt{\frac{4}{3}}$ and infinity.

The Lamb mode dispersion curves for the full allowed range of Poisson's ratio are examined in the next section.

4.2 TYPE F Intersections

Following [6], the type F intersections of Lamb mode dispersion curve requires

$$F^{\pm}(\Omega, \kappa) = 1, \tag{4.2.1}$$

$$\Rightarrow \frac{4\kappa^2 \sqrt{(\Omega^2 - \kappa^2)(\frac{\Omega^2}{e^2} - \kappa^2)}}{(\Omega^2 - 2\kappa^2)^2} = 1,$$

$$\Rightarrow 4\kappa^2 \sqrt{(\Omega^2 - \kappa^2)(\frac{\Omega^2}{e^2} - \kappa^2)} = (\Omega^2 - 2\kappa^2)^2,$$

$$\Rightarrow 4\kappa^4 \sqrt{(\frac{\Omega^2}{\kappa^2} - 1)(\frac{\Omega^2}{\kappa^2 e^2} - 1)} = \kappa^4 (\frac{\Omega^2}{\kappa^2} - 2)^2,$$

where for $\nu = \frac{\Omega}{\kappa} = \frac{1}{c_T}\frac{\omega}{\kappa}$, we get

$$(\nu^2 - 2)^2 = 4\sqrt{(\nu^2 - 1)(\frac{\nu^2}{e^2} - 1)}. \tag{4.2.2}$$

Equation (4.2.2) is the well known relation used to find out the Rayleigh wave velocity $V_R = \nu c_T$ of a material and shows that the Rayleigh equation can be cast in the form of a cubic equation in ν^2 having three solution. From [10], it follows that one of the solutions for allowed e is always real, positive, and less than unity, and corresponds to the Rayleigh velocity.

No Type F intersections exist for $e > 1.76364$ because it is obvious from Eq (4.2.2) that the additional solution for ν will be complex yielding no real intersection. For $\sqrt{\frac{4}{3}} < e < 1.76364$, these additional solutions are real and leads to real intersection. From Eq (4.2.1) we get the following condition to get the location of type F intersection points

$$\frac{\tan(\frac{\pi}{2}\sqrt{\nu^2 - 1}\kappa)}{\tan(\frac{\pi}{2}\sqrt{\frac{\nu^2}{e^2} - 1}\kappa)} + 1 = 0,$$

$$\Rightarrow \tan(\frac{\pi}{2}\sqrt{\nu^2 - 1}\kappa) + \tan(\frac{\pi}{2}\sqrt{\frac{\nu^2}{e^2} - 1}\kappa) = 0,$$

$$\Rightarrow \frac{\sin(\frac{\pi}{2}\sqrt{\nu^2 - 1}\kappa)}{\cos(\frac{\pi}{2}\sqrt{\nu^2 - 1}\kappa)} + \frac{\sin(\frac{\pi}{2}\sqrt{\frac{\nu^2}{e^2} - 1}\kappa)}{\cos(\frac{\pi}{2}\sqrt{\frac{\nu^2}{e^2} - 1}\kappa)} = 0,$$

$$\Rightarrow \sin(\frac{\pi}{2}\sqrt{\nu^2 - 1}\kappa)\cos(\frac{\pi}{2}\sqrt{\frac{\nu^2}{e^2} - 1}\kappa) + \sin(\frac{\pi}{2}\sqrt{\frac{\nu^2}{e^2} - 1}\kappa)\cos(\frac{\pi}{2}\sqrt{\nu^2 - 1}\kappa) = 0.$$

Using the formula $\sin(\alpha + \beta) = \sin\alpha\cos\beta + \cos\alpha\sin\beta$ above, we get

$$\sin(\frac{\pi}{2}\kappa(\sqrt{\nu^2 - 1} + \sqrt{\frac{\nu^2}{e^2} - 1})) = 0,$$

22

$$\Rightarrow (\frac{\pi}{2}\kappa(\sqrt{\nu^2 - 1} + \sqrt{\frac{\nu^2}{e^2} - 1})) = z\pi,$$

$$\Rightarrow \kappa = \frac{2z}{\sqrt{\nu^2 - 1} + \sqrt{\frac{\nu^2}{e^2} - 1}}; \qquad \Omega = \nu\kappa, \qquad (4.2.3)$$

where z is a positive integer. Equation (4.2.3) thus gives the location of intersection points for type F intersections.

4.3 TYPE I and TYPE II Intersections

The two conditions under which the symmetric and antisymmetric dispersion curves intersect will be referred as Type I and Type II intersections. If the tangent functions in Eq (4.1.1) are simultaneously infinite then these intersections are referred as Type I while if the tangent functions are simultaneously zero then will be referred as Type II intersections. The solutions of Eq (4.1.1) at these intersection points exist only in the limiting sense of L'Hospital's rule. The condition below holds simultaneously for Type I and Type II intersection

$$\sqrt{\Omega^2 - \kappa^2} = n,$$

$$\sqrt{\frac{\Omega^2}{e^2} - \kappa^2} = m, \qquad (4.3.1)$$

where n and m are positive odd integers for Type I intersection while n and m are positive even integers for Type II intersection.

We will use Eq (4.3.1) to get the intersection point for both types. So we have

$$\Omega^2 - \kappa^2 = n^2,$$

$$\Rightarrow \kappa^2 = \Omega^2 - n^2,$$

$$\Rightarrow \kappa = \sqrt{\Omega^2 - n^2}. \qquad (4.3.2)$$

Similarly

$$\frac{\Omega^2}{e^2} - \kappa^2 = m^2,$$

$$\Rightarrow \Omega^2 - e^2\kappa^2 = e^2 m^2. \qquad (4.3.3)$$

By putting Eq (4.3.2) in (4.3.3), we get

$$\Omega^2 - e^2(\Omega^2 - n^2) = e^2 m^2,$$

23

$$\Rightarrow \Omega^2(1-e^2) = e^2m^2 - e^2n^2,$$

$$\Rightarrow \Omega^2 = \frac{e^2n^2 - e^2m^2}{e^2 - 1},$$

$$\Rightarrow \Omega = e\sqrt{\frac{n^2 - m^2}{e^2 - 1}}. \tag{4.3.4}$$

Substituting Eq (4.3.4) in (4.3.2), we get

$$\kappa = \sqrt{\frac{e^2n^2 - e^2m^2}{e^2 - 1} - n^2},$$

$$\Rightarrow \kappa = \sqrt{\frac{e^2n^2 - e^2m^2 - e^2n^2 + n^2}{e^2 - 1}},$$

$$\Rightarrow \kappa = \sqrt{\frac{n^2 - e^2m^2}{e^2 - 1}}. \tag{4.3.5}$$

So for either type, the intersection point is located at

$$\kappa_{nm} = \sqrt{\frac{n^2 - e^2m^2}{e^2 - 1}}, \tag{4.3.6}$$

$$\Omega_{nm} = e\sqrt{\frac{n^2 - m^2}{e^2 - 1}}, \tag{4.3.7}$$

where $n > em$ and $n > m$ for the real solution of κ_{nm} and Ω_{nm}.

At the crossing points the phase velocity of modes is given by:

$$V_{nm}^p = c_T \frac{\Omega_{nm}}{\kappa_{nm}},$$

$$= c_T \frac{e\sqrt{\frac{n^2 - m^2}{e^2 - 1}}}{\sqrt{\frac{n^2 - e^2m^2}{e^2 - 1}}},$$

$$\Rightarrow V_{nm}^p = c_T e\sqrt{\frac{n^2 - m^2}{n^2 - e^2m^2}}. \tag{4.3.8}$$

Moreover, we will use Eq (4.3.6) and (4.3.7) to find the value of $F(\Omega, \kappa)$ at the intersection of modes

$$F(\Omega, \kappa) = \frac{4\left(\frac{n^2 - e^2m^2}{e^2 - 1}\right)\sqrt{\left(\frac{e^2n^2 - e^2m^2}{e^2 - 1} - \frac{n^2 - e^2m^2}{e^2 - 1}\right)\left(\frac{e^2n^2 - e^2m^2}{e^2(e^2 - 1)} - \frac{n^2 - e^2m^2}{e^2 - 1}\right)}}{\left(\frac{e^2n^2 - e^2m^2}{e^2 - 1} - 2\left(\frac{n^2 - e^2m^2}{e^2 - 1}\right)\right)^2},$$

$$= \frac{4(n^2 - e^2m^2)\sqrt{(e^2n^2 - e^2m^2 - n^2 + e^2m^2)(n^2 - m^2 - n^2 + e^2m^2)}}{(e^2n^2 - e^2m^2 - 2(n^2 - e^2m^2))^2},$$

$$= \frac{4(n^2 - e^2m^2)\sqrt{n^2m^2(e^2 - 1)^2}}{(e^2m^2 + n^2(e^2 - 2))^2},$$

$$\Rightarrow F(\Omega, \kappa) = \frac{4nm(e^2 - 1)(n^2 - e^2m^2)}{(n^2(e^2 - 2) + e^2m^2)^2}.$$

Graphically the symmetric and antisymmetric Lamb modes when separately presented gives a family of curves, none of which crosses the other. But for some special values of e there exist some points where they may cross each other.

For aluminum with $e = 2.0288$, no Type F intersections exist. The value of e for aluminum is greater than 1.76364, so there exist no real intersections between dispersion curves. Type I and Type II intersections are labeled according to n, m values calculated from Eq (4.3.6) and (4.3.7) with n, m odd integers for Type I and even integers for Type II intersection. In figure (4.1), we observed the near intersection between symmetric and antisymmetric modes at points $\Omega = 4$ and $\Omega = 8$. While at $\Omega = 2$ and $\Omega = 6$ intersection and near intersection for symmetric modes are observed.

The figure (4.1) shows the intersection between symmetric and antisymmetric Lamb modes for aluminum plate presented by [6]:
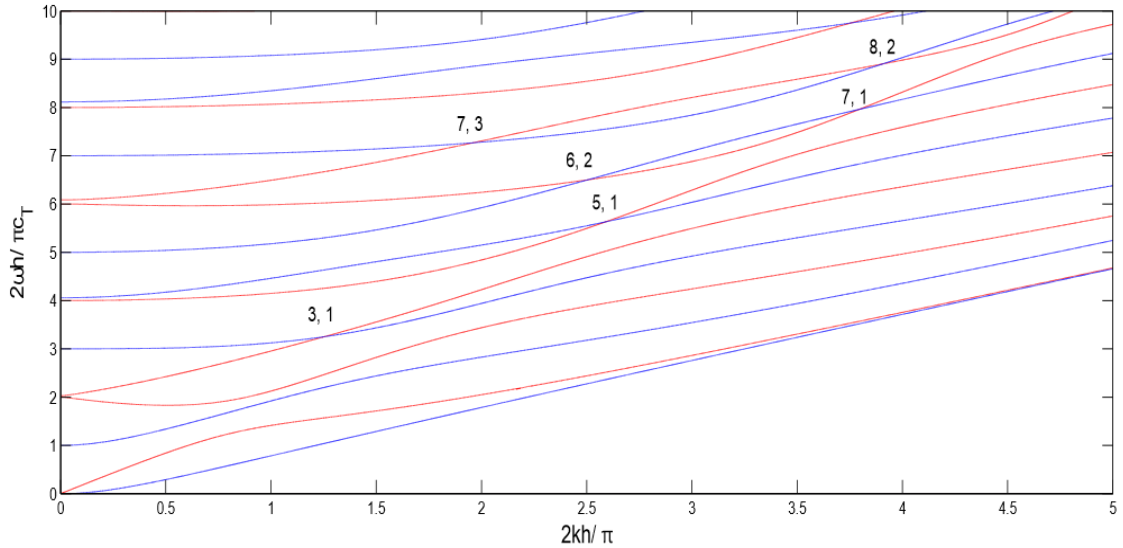

Figure 4.1: Intersection between symmetric and antisymmetric Lamb modes for an aluminum plate of $e = 2.0288 \geq 1.76364$ in $k - \Omega$ plane with no Type F intersections. Type I and Type II intersections are labeled according to the values of n, m with n and m being positive odd integers for Type I intersection and positive even integers for Type II intersection. Here (3, 1), (5, 1), (7, 1), (7, 3) are Type I intersection points while (6, 2) and (8, 2) are Type II intersection points.

For beryllium plate with $e = 1.45$, type F intersections exist and are labeled according with the value of z calculated from Eq (4.2.3). The line F_1 having slope 1.4500045 and the line F_2 with slope 2.262 has uniformly spaced sequences of Type F, labeled according to the values of z. Type I and Type II intersections are labeled according to n, m values calculated from Eq (4.3.6) and (4.3.7) with n, m odd integer for Type I and n, m even integer for Type II intersection. There exist some points in fig (4.2) where near intersections between symmetric modes exist and are labeled as a_1, a_2 and a_3.

The figure (4.2) shows the intersection between symmetric and antisymmetric Lamb modes for beryllium plate given by [6]:
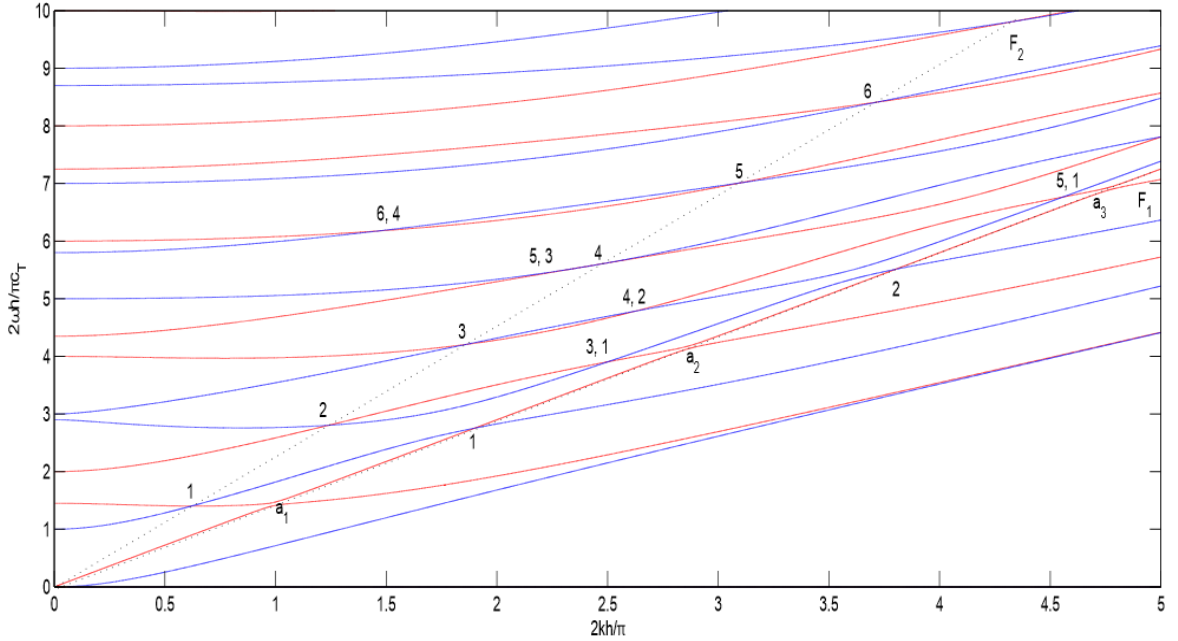

Figure 4.2: Intersection between symmetric and antisymmetric Lamb modes for beryllium plate of $e = 1.45$ in $k - \Omega$ plane. The intersection points on line F_1 are labeled as 1, 2 and F_2 as 1, 2, 3, 4, 5, 6 according to the value of z calculated from Eq (4.2.3); a_1, a_2 and a_3 are near intersection points. Type I and Type II are labeled according to the value of n, m with n and m being positive odd integers for Type I intersection and positive even integers for Type II intersection. Here (3, 1), (5, 3) and (5, 1) are Type I intersection points while (4, 2) and (6, 4) are Type II intersection points.

For an auxetic material with $e = 1.3$, type F intersections exist and are labeled according with the value of z calculated from Eq (4.2.3). The line F_1 having slope 1.4500045 and the line F_2 with slope 2.262 has uniformly spaced sequences of Type F, labeled according to the values of z. Type I and Type II intersections are labeled according to n, m values calculated from Eq (4.3.6) and (4.3.7) with n, m odd integer for Type I and n, m even integer for Type II intersection. The figure (4.3) shows the intersection between symmetric and antisymmetric Lamb modes for an auxetic material is given by [6]:
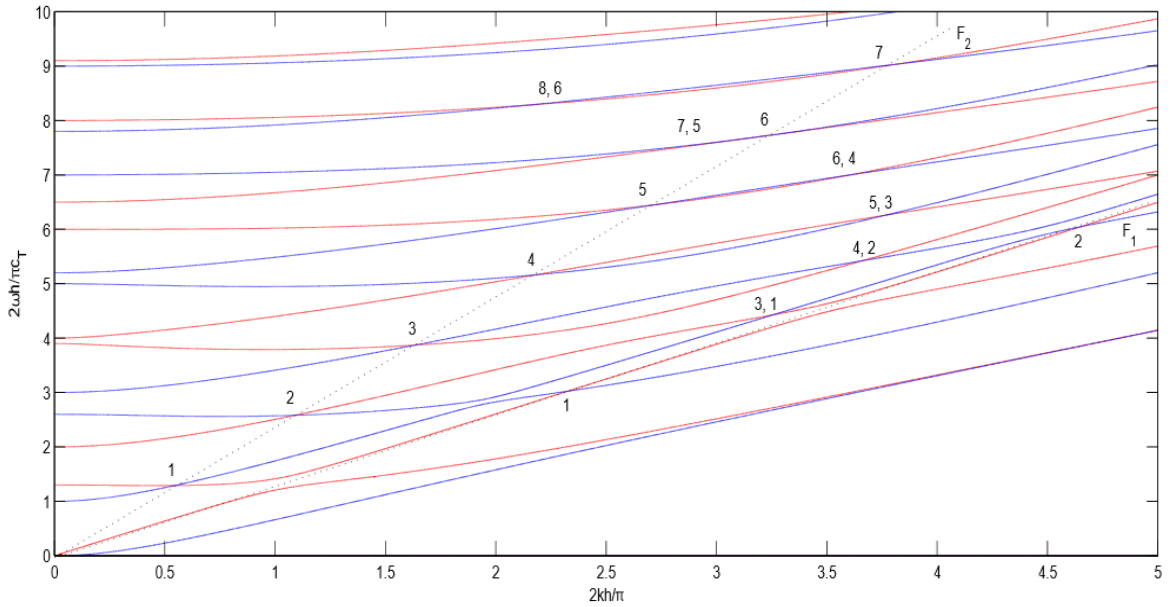

Figure 4.3: Intersection between symmetric and antisymmetric Lamb modes for an auxetic material which have negative value of σ with $e = 1.3$ in $k - \Omega$ plane. The intersection points on line F_1 are labeled as 1, 2 and F_2 as 1, 2, 3, 4, 5, 6, 7 according to the value of z calculated from Eq (4.2.3). Type I and Type II are labeled according to the value of n, m with n and m being positive odd integers for Type I intersection and positive even integers for Type II intersection. Here (3, 1), (5, 3) and (7, 5) are Type I intersection points while (4, 2), (6,4) and (8, 6) are Type II intersection points.

4.4   Evaluation of intersection points in k-c plane

By using normalized frequency and normalized wave number respectively MAT-LAB environment is used to find the intersection points of symmetric and anti-symmetric lamb modes.

The figure (4.4) depicts the intersections between symmetric and antisymmetric Lamb modes for aluminum plate with no type F intersections. Type I and Type II intersections are labeled according to n, m values calculated from Eq (4.3.6) and (4.3.7) with n, m odd integer for Type I and even for Type II intersections.
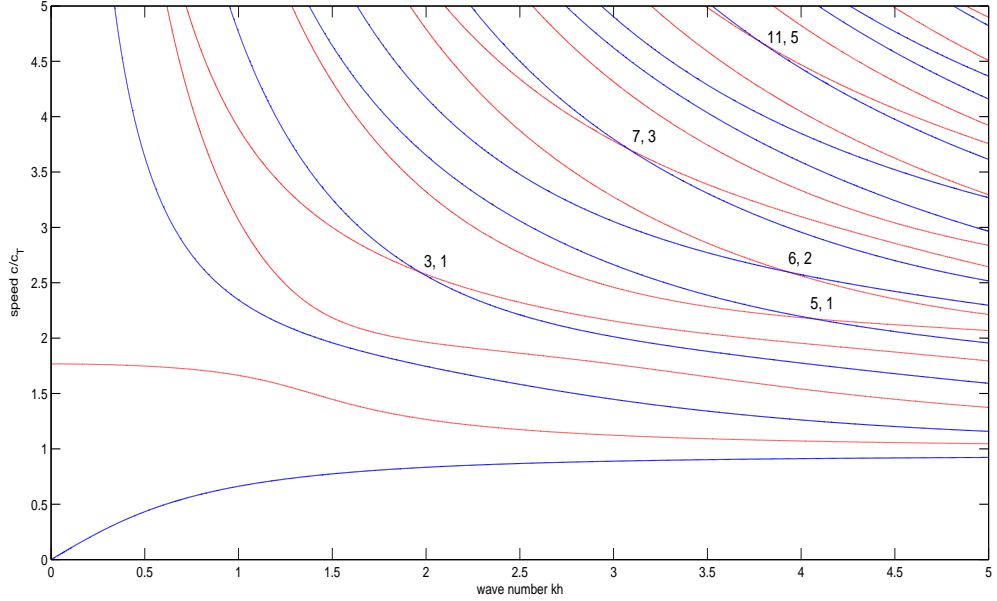

Figure 4.4: Intersection between symmetric and antisymmetric Lamb modes for an aluminum plate with $e = 2.0288$ in $k - c$ plane with no Type F intersections. Type I and Type II are labeled according to the value of n, m with n and m being positive odd integers for Type I intersection and positive even integers for Type II intersection. Here (3, 1), (5, 1), (7, 3) and (11, 5) are Type I intersection points while (6, 2) is Type II intersection point.

The figure (4.5) shows the intersection between symmetric and antisymmetric Lamb modes for beryllium plate. Type F intersections exist and are labeled according with the value of z calculated from equation (4.2.3). Type I and Type II intersections are labeled according to n, m values calculated from Eq (4.3.6) and (4.3.7) with n, m odd integer for Type I and even for Type II intersections.
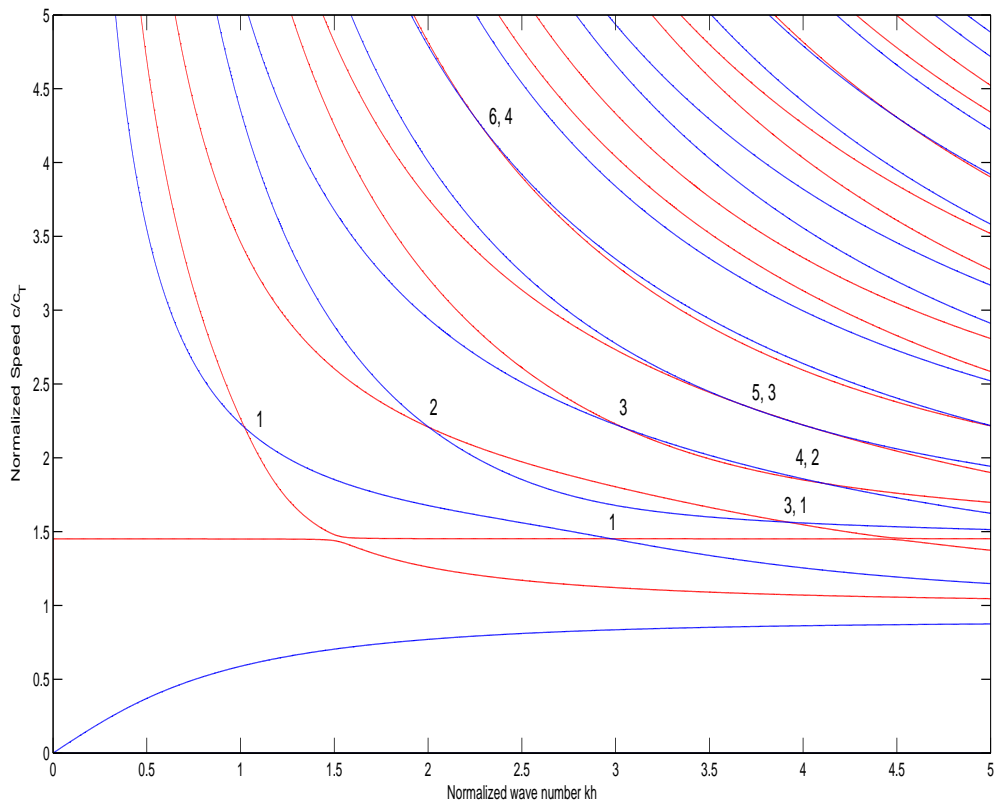

Figure 4.5: Intersection between symmetric and antisymmetric Lamb modes for beryllium plate with $e = 1.45$ in $k - c$ with Type F intersections labeled as 1, 2, 3 according to the value of z calculated from Eq (4.2.3). Type I and Type II are labeled according to the value of n, m with n and m being positive odd integers for Type I intersection and positive even integers for Type II intersection. Here (3, 1) and (5, 3) are Type I intersection points while (4, 2) and (6, 4) are Type II intersection points.

The figure (4.6) shows the intersection between symmetric and antisymmetric Lamb modes for an auxetic material having negative Poisson's ratio with $e = 1.3$. Type F intersections exist and are labeled according with the value of z calculated from Eq (4.2.3). Type I and Type II intersections are labeled according to n, m values calculated from Eq (4.3.6) and (4.3.7) with n, m odd integer for Type I and even integer for Type II intersection.
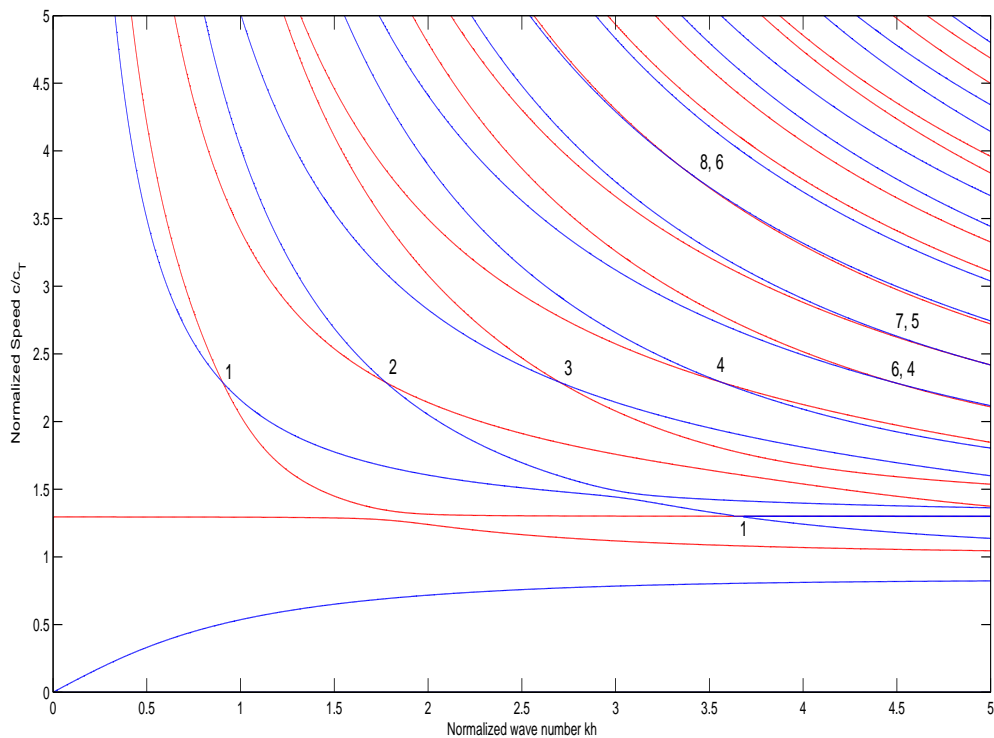

Figure 4.6: Intersection between symmetric and antisymmetric Lamb modes for an auxetic material with $e = 1.3$ in $k - c$ with Type F intersections labeled as 1, 2, 3, 4 according to the value of z calculated from Eq (4.2.3). Type I and Type II are labeled according to the value of n, m with n and m being positive odd integers for Type I intersection and positive even integers for Type II intersection. Here $(7, 5)$ is Type I intersection point while $(6, 4)$ and $(8, 6)$ are Type II intersection points.

4.5   Plateau region for Lamb modes

The Rayleigh-Lamb frequency relation for Lamb modes demonstrates that the slope of a mode vanishes at some points giving rise to plateau region.

By using equation (4.1.1), MATLAB environment is used to find the plateau region for different materials.

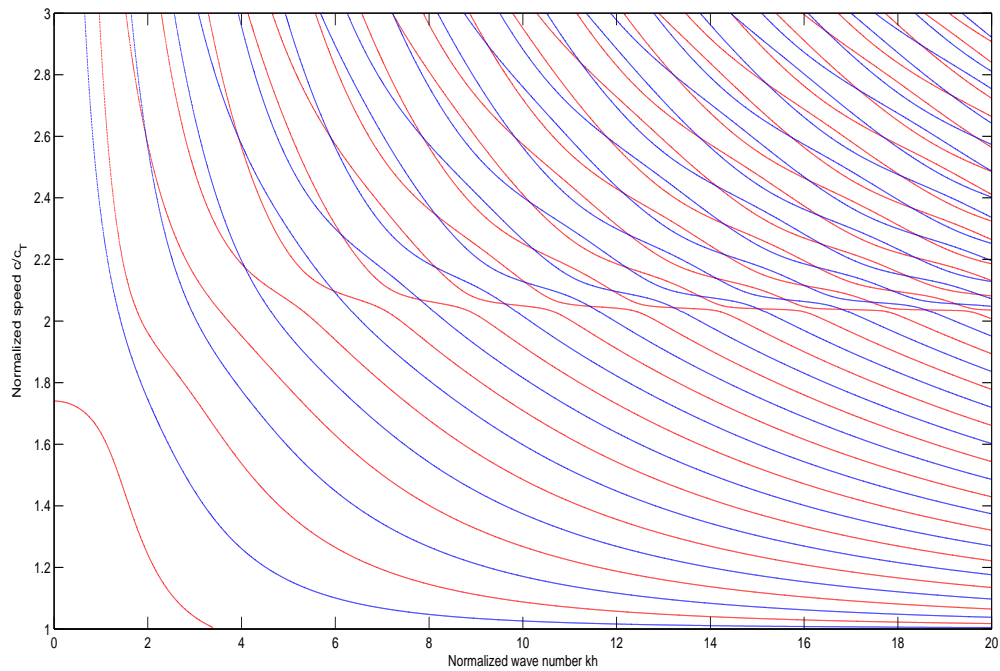Figure (4.7) is the graphical representation of an aluminum plate with plateau region:

Figure 4.7: Plateau region for aluminum plate.

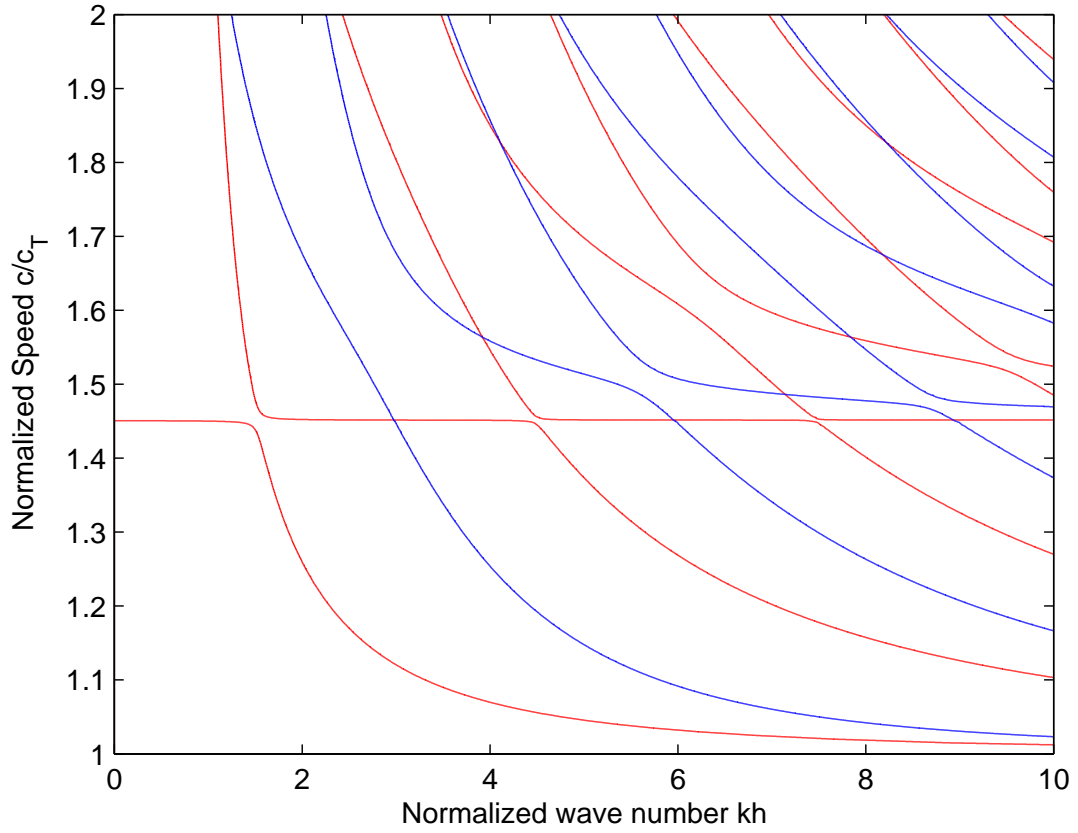The figure (4.8) is the graphical representation of beryllium plate with plateau region:

Figure 4.8: Plateau region for beryllium plate.

The figure (4.9) is the graphical representation of an auxetic material with plateau region:
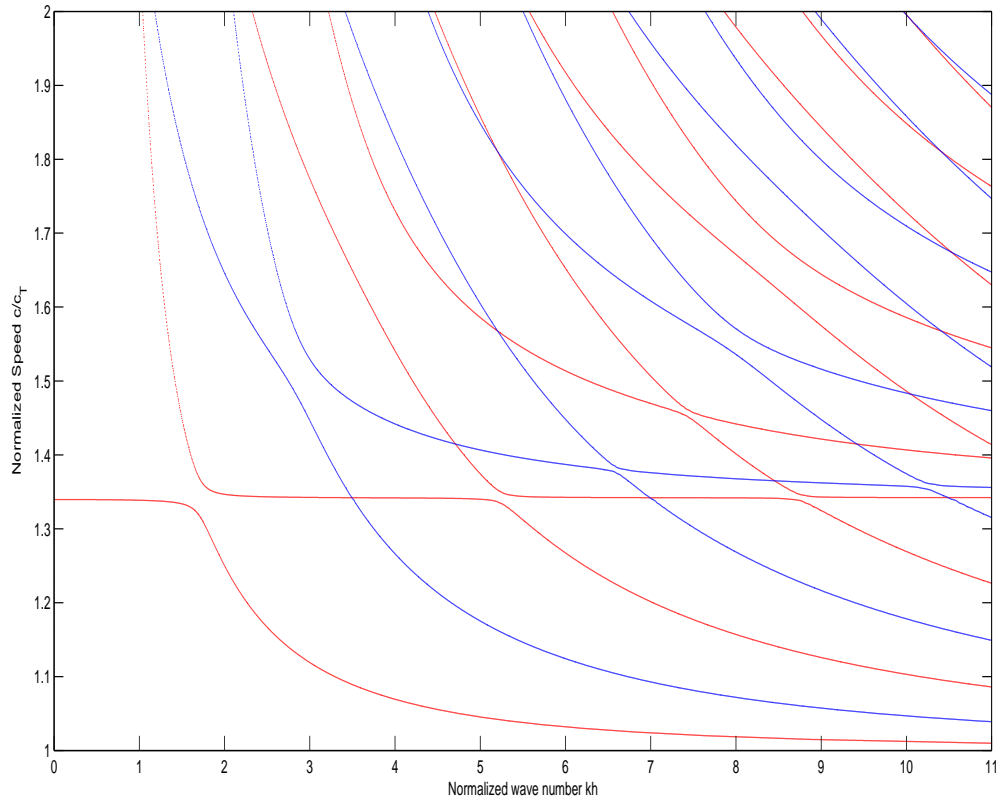

Figure 4.9: Plateau region for an auxetic material.

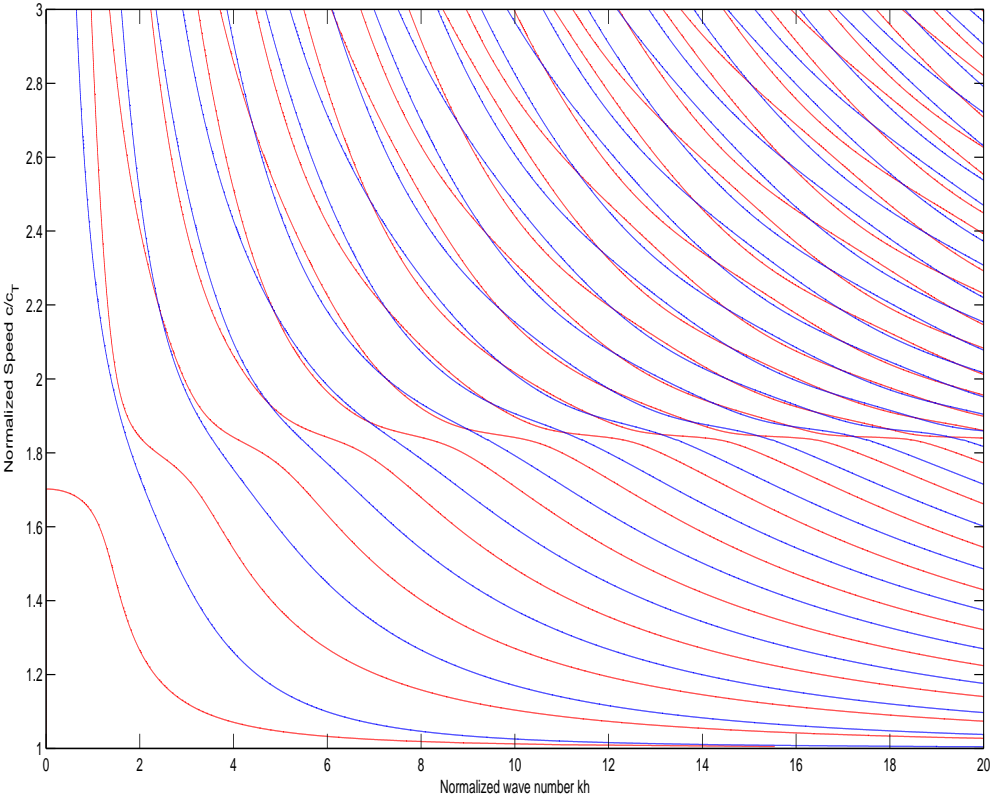The figure (4.10) is the graphical representation of steel with plateau region:

Figure 4.10: Plateau region for steel.

Chapter 5

Mode conversion due to reflection

A plane usually divides the three-dimensional Euclidean space into two sections, among which either of one section is termed as half space. When a wave reflects in a half space, one form of wave energy can be transformed into another form and this phenomena is referred as mode conversion. An SV wave can be converted to a P wave after reflection from the boundary of a half space with a properly chosen angle of incidence.

In this chapter, mode conversion of an incident SV-wave is studied in a half space. An incident SV-wave reflects as an SV-wave and a P-wave. Also an analytical expression in e is derived to find the bound in which mode conversion can take place and outside which it is forbidden.

5.1 Introduction

Consider a half space with $x_1 \geq 0$, x_2-axis normal to it and $x_2{=}0$ is the boundary of half space while $x_2 \leq 0$ is occupied by an elastic material and $x_2 > 0$ is vacuum. Consider a wave traveling in the half space with a wave vector $\boldsymbol{n}$. We choose x_1-axis so that $\boldsymbol{n}$ is in the x_1-x_2 plane. The wave is described by the plane harmonic displacement vector:

$$\boldsymbol{u} = A\boldsymbol{p}e^{ik(\boldsymbol{n}.\boldsymbol{x}-ct)}, \tag{5.1.1}$$

where $\boldsymbol{p}$ is the polarization vector, k is wave number, c is the speed of wave and A is the amplitude of wave respectively. There are two types of plane harmonic wave:

1) Longitudinal wave for $\boldsymbol{n}=\boldsymbol{p}$.

2) Transverse wave for $\boldsymbol{n} \perp \boldsymbol{p}$.

2a) When $\boldsymbol{p} = (0, 0, 1)$ is called SH-wave.

2b) When $\boldsymbol{p} \perp \boldsymbol{n}$ but in the x_1-x_2 plane is called SV-wave.

Boundary Conditions

On the free boundary the displacement due to wave motion produces stress, τ_{ij}, since stress is caused by an elastic material on the positive side of a surface element acting on the material, so on the other side $\tau_{ij} = 0$. Therefore, stress is zero while displacement is non-zero on the free boundary.

5.2 Reflection of SV-waves

Following [9], to examine the reflection of SV waves, considered an SV wave propagating in a half space characterized by the respective speeds c_T and c_L of an S wave and a P wave. The incident SV wave reflects partly as a P wave and partly as an SV wave.

Let θ_o be the angle of incidence of an SV-wave and θ_1 , θ_2 be the angles of reflection of the P and SV-wave. Also let A_o be the amplitude of an incident SV wave and A_1 , A_2 be the amplitudes of the reflected P and SV waves respectively. The figure (5.1) shows the reflection of SV-wave in a half space:
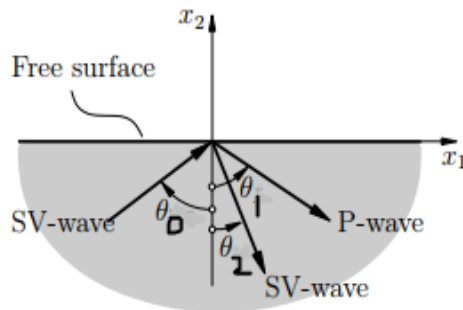

Figure 5.1: Reflection of SV wave.

36

The displacement vector of the incident SV-wave in the plane $x_2 = 0$ is of the form

$$\boldsymbol{u}^{(0)} = A_0 \boldsymbol{p} e^{ik_0(\boldsymbol{n_0}.\boldsymbol{x} - c_T t)},$$

where $\boldsymbol{n}_0 = (\sin\theta_0, \cos\theta_0, 0)$.

While for reflected P-wave and SV-wave displacement vector is given by

$$\boldsymbol{u}^{(1)} = A_1 \boldsymbol{p} e^{ik_1(\boldsymbol{n_1}.\boldsymbol{x} - c_L t)},$$
$$\boldsymbol{u}^{(2)} = A_2 \boldsymbol{p} e^{ik_2(\boldsymbol{n_2}.\boldsymbol{x} - c_T t)},$$

where $\boldsymbol{n}_1 = (\sin\theta_1, -\cos\theta_1, 0)$ and $\boldsymbol{n}_2 = (\sin\theta_2, -\cos\theta_2, 0)$.

We will consider only the case when the reflecting surface is free of tractions at $x_2 = 0$. The stress on such a surface is given by

$$\tau_{21} = 0,$$

$$\tau_{21}^{(0)} + \tau_{21}^{(1)} + \tau_{21}^{(2)} = 0,$$

$$ik_0\mu(\sin^2\theta_0 - \cos^2\theta_0)A_0 \exp^{ik_0(\sin\theta_0.\boldsymbol{x_1} - c_T t)})$$
$$-2ik_1\mu\sin\theta_1\cos\theta_1 A_1 \exp^{ik_1(\sin\theta_1.\boldsymbol{x_1} - c_L t)}$$
$$-ik_2\mu(\sin^2\theta_2 - \cos^2\theta_2)A_2 \exp^{ik_2(\sin\theta_2.\boldsymbol{x_1} - c_T t)} = 0. \qquad (5.2.1)$$

Similarly

$$\tau_{22} = 0,$$

$$\tau_{22}^{(0)} + \tau_{22}^{(1)} + \tau_{22}^{(2)} = 0,$$

$$2ik_0\mu\sin\theta_0\cos\theta_0 A_0 \exp^{ik_0(\sin\theta_0.\boldsymbol{x_1} - c_T t)}$$
$$+ik_1(\lambda + 2\mu\cos^2\theta_1)A_1 \exp^{ik_1(\sin\theta_1.\boldsymbol{x_1} - c_L t)}$$
$$-2ik_2\mu\sin\theta_2\cos\theta_2 A_2 \exp^{ik_2(\sin\theta_2.\boldsymbol{x_1} - c_T t)} = 0. \qquad (5.2.2)$$

The exponentials must vanish in (5.2.1) and (5.2.2), which gives

$$k_0 c_T = k_1 c_L = k_2 c_T,$$

$$k_0 \sin\theta_0 = k_1 \sin\theta_1 = k_2 \sin\theta_2,$$

which yields

$$k_0 = k_2, \tag{5.2.3}$$

$$\Rightarrow \frac{k_0}{k_1} = \frac{c_L}{c_T} = e, \tag{5.2.4}$$

and

$$\theta_2 = \theta_0, \tag{5.2.5}$$

$$\sin \theta_1 = \frac{k_0}{k_1} \sin \theta_0 = e \sin \theta_0. \tag{5.2.6}$$

By using (5.2.3)-(5.2.6) in (5.2.1) and (5.2.2), the following set of equations for $\frac{A_1}{A_0}$ and $\frac{A_2}{A_0}$ are obtained

$$(\lambda + 2\mu \cos^2 \theta_1)(\frac{A_1}{A_0}) - e\mu \sin 2\theta_0 (\frac{A_2}{A_0}) = -e\mu \sin 2\theta_0.$$

$$-\mu \sin 2\theta_1 (\frac{A_1}{A_0}) - e\mu \cos 2\theta_0 (\frac{A_2}{A_0}) = e\mu \cos 2\theta_0.$$

The solutions to this set of equations are

$$\frac{A_1}{A_0} = -\frac{e \sin 4\theta_0}{\sin 2\theta_0 \sin 2\theta_1 + e^2 \cos^2 2\theta_0}. \tag{5.2.7}$$

$$\frac{A_2}{A_0} = \frac{\sin 2\theta_0 \sin 2\theta_1 - e^2 \cos^2 2\theta_0}{\sin 2\theta_0 \sin 2\theta_1 + e^2 \cos^2 2\theta_0}. \tag{5.2.8}$$

In the expression for $\frac{A_1}{A_0}$, the reflected P-wave vanishes for $\theta_0 = 0$, $\theta_0 = \frac{\pi}{4}$, $\theta_0 = \frac{\pi}{2}$. For these specific values incident SV-wave reflects as an SV-wave while if the numerator of (5.2.8) vanishes then incident SV-wave reflects as a P-wave.

5.3   Mode conversion through reflection

To find out the bound for mode conversion consider Eq (5.2.6), (5.2.7) and (5.2.8). From Eq (5.2.6) it follows that θ_1 must be a real-valued angle and it is possible only if θ_o is smaller than or equal to the critical angle θ_{c_T} given by

$$\theta_o \leq \theta_{c_T},$$

where critical angle θ_{c_T} is given by

$$\theta_{c_T} = \sin^{-1}(\frac{1}{e}).$$

Let the cross-sectional area of incident SV-waves is denoted by ΔS_o and the cross-sectional area of reflected P-wave and SV-wave is denoted by ΔS_1 and ΔS_2. The average energy transmission across ΔS_o must be equal to the sum of average energy transmissions across ΔS_1 and ΔS_2 because the surface area ΔS is free of tractions and no energy is dissipated. Using the energy transmission relation for longitudinal and transverse waves given by [9],

$$p_L = \frac{1}{2}(\lambda + 2\mu)\frac{\omega^2 A^2}{c_L},$$

$$p_T = \frac{1}{2}\mu\frac{\omega^2 A^2}{c_T},$$

where p_L and p_T are energy transmission of longitudinal and transverse waves, so average energy transmission relation is given by

$$\frac{1}{2}\mu\frac{\omega^2}{c_T}(A_o)^2\Delta S_o = \frac{1}{2}(\lambda + 2\mu)\frac{\omega^2}{c_L}(A_1)^2\Delta S_1 + \frac{1}{2}\mu\frac{\omega^2}{c_T}(A_2)^2\Delta S_2.$$

By using

$$\Delta S_o = \Delta S_2 = \Delta S \cos\theta_o \ , \quad \Delta S_1 = \Delta S \cos\theta_1$$

Further simplification leads to the following equation

$$(\frac{A_1}{A_o})^2\frac{\cos\theta_1}{\cos\theta_o}e + (\frac{A_2}{A_o})^2 = 1. \tag{5.3.1}$$

Suppose for $\theta_o = \alpha$, the right hand side of Eq (5.2.8) vanishes. This will imply that an SV-wave with an angle of incident α is reflected as a P-wave giving rise to *mode conversion* phenomena.

Let

$$f(\theta_o) = \sin 2\theta_o \sin 2\theta_1 - e^2 \cos^2 2\theta_o. \tag{5.3.2}$$

For $\theta_o=0$ in (5.3.2), we have

$$f(0) = -e^2 < 0,$$

and for $\theta_o = \theta_{c_T}$ in (5.3.2), leads to

$$f(\theta_{c_T}) = 2 - e^2 < 0.$$

So it follows that either $f(\theta_o)$ does not vanish at all in $[0, \theta_{c_T}]$ or it has at least two zeros in the interval. Thus if mode conversion occurs, it does more than once as we increase the angle of incidence from zero to θ_{c_T}.

5.4 An inequality for e

As we are familiar with the following expression below

$$e^2 = \frac{\lambda + 2\mu}{\mu},$$

$$\Rightarrow e = \sqrt{\frac{\lambda + 2\mu}{\mu}},$$

$$\Rightarrow e = \sqrt{\frac{\lambda}{\mu} + 2},$$

which shows that

$$e > \sqrt{2},$$

it gives a lower bound for mode conversion.

Now we will proceed to get the upper bound for mode conversion.

Suppose the right hand side of Eq (5.2.8) vanishes for $\theta_o = \alpha$, then we have

$$\sin 2\alpha \sin 2\alpha_1 - e^2 \cos^2 2\alpha = 0,$$

$$\sin 2\alpha \sin 2\alpha_1 = e^2 \cos^2 2\alpha, \tag{5.4.1}$$

where α_1 is defined through the relation $\sin \alpha_1 = e \sin \alpha$. Substituting Eq (5.4.1) in (5.2.7) gives

$$\frac{A_1}{A_o} = -\frac{e \sin 4\alpha}{2e^2 \cos^2 2\alpha},$$

$$\frac{A_1}{A_o} = -\frac{e(2 \sin 2\alpha \cos 2\alpha)}{2e^2 \cos^2 2\alpha},$$

so we get

$$\frac{A_1}{A_o} = -\frac{\tan 2\alpha}{e}.$$

Putting the above expression in (5.3.1), we get

$$\left(\frac{\tan 2\alpha}{e}\right)^2 \frac{\cos \alpha_1}{\cos \alpha_o} e + \left(\frac{A_2}{A_o}\right)^2 = 1,$$

where $\frac{A_2}{A_o} = 0$ due to mode conversion, so we are left with

$$\left(\frac{\tan 2\alpha}{e}\right)^2 \frac{\cos \alpha_1}{\cos \alpha} e = 1,$$

$$\frac{(\tan 2\alpha)^2 \cos \alpha_1}{\cos \alpha} = e. \tag{5.4.2}$$

Now we will proceed to get an expression for tan2α and $\frac{\cos \alpha_1}{\cos \alpha}$ in e.

Since, angle of incidence must be less than or equal to the critical angle, therefore

$$\alpha \leq \sin^{-1} \frac{1}{e},$$

$$\Rightarrow \sin \alpha \leq \frac{1}{e}. \tag{5.4.3}$$

We know that

$$\sin^2 \alpha + \cos^2 \alpha = 1,$$

$$\cos^2 \alpha = 1 - \sin^2 \alpha,$$

$$\cos \alpha = \sqrt{1 - \sin^2 \alpha}.$$

Using (5.4.3), we get

$$\cos \alpha \geq \frac{\sqrt{e^2 - 1}}{e}. \tag{5.4.4}$$

From (5.4.3) and (5.4.4), we have

$$\tan \alpha \leq \frac{1}{\sqrt{e^2 - 1}}. \tag{5.4.5}$$

It is well known that

$$\tan 2\alpha = \frac{2 \tan \alpha}{1 - \tan^2 \alpha}. \tag{5.4.6}$$

By using (5.4.5) in Eq (5.4.6) yields

$$\tan 2\alpha \leq \frac{2\sqrt{e^2 - 1}}{e^2 - 2}. \tag{5.4.7}$$

Similarly to get an expression in e for $\frac{\cos \alpha_1}{\cos \alpha}$, we will differentiate Eq (5.3.2) and get

$$f'(\alpha) = 2 \cos 2\alpha \sin 2\alpha_1 + 2 \sin 2\alpha \cos 2\alpha_1 \frac{d\theta_1}{d\theta_o} + 4e^2 \cos 2\alpha \sin 2\alpha. \tag{5.4.8}$$

Taking derivative of Eq (5.2.6), we get

$$\frac{d\theta_1}{d\theta_o} = e \frac{\cos \theta_o}{\cos \theta_1}.$$

By putting value of $\frac{d\theta_1}{d\theta_o}$ in (5.4.8) gives

$$f'(\alpha) = 2 \cos 2\alpha \sin 2\alpha_1 + 2e \sin 2\alpha \cos 2\alpha_1 \frac{\cos \alpha}{\cos \alpha_1} + 4e^2 \cos 2\alpha \sin 2\alpha. \tag{5.4.9}$$

41

Since
$$e > \sqrt{2},$$

and
$$\sin \alpha \leq \frac{1}{e}, \tag{5.4.10}$$

which implies that
$$\alpha < \frac{\pi}{4}.$$

The observation that $f(\theta_o)$ vanishes more than once leads to the conclusion that the right hand side of Eq (5.4.9) must be negative for the largest zero of Eq (5.3.2). This is possible only if the middle term of Eq (5.4.9) is negative.
Hence
$$\alpha_1 > \frac{\pi}{4}, \tag{5.4.11}$$

$$\Rightarrow \sin \alpha_1 > \frac{1}{\sqrt{2}}.$$

From (5.2.6) and the above result, we get
$$\Rightarrow \sin \alpha > \frac{1}{\sqrt{2}e}.$$

Also we have
$$\sin \alpha \leq \frac{1}{e},$$

which implies
$$\frac{1}{\sqrt{2}e} < \sin \alpha \leq \frac{1}{e}. \tag{5.4.12}$$

As from (5.4.1), we have
$$\sin 2\alpha \sin 2\alpha_1 = e^2 \cos^2 2\alpha,$$

$$\sin 2\alpha \sin 2\alpha_1 = e^2 (2\cos^2 \alpha - 1)^2.$$

By using (5.4.4) in above equation, we find
$$\sin 2\alpha \sin 2\alpha_1 \leq \frac{(e^2 - 2)^2}{e^2}, \tag{5.4.13}$$

now by using the formula $\sin 2\theta = 2 \sin \theta \cos \theta$ in above inequality, which gives
$$\cos \alpha \cos \alpha_1 \geq \frac{(e^2 - 2)^2}{4e^2 \sin \alpha \sin \alpha_1},$$

42

$$\cos\alpha\cos\alpha_1 < \frac{(e^2-2)^2}{2e}, \tag{5.4.14}$$

where we have used (5.4.11) and (5.4.12) to obtain the last inequality.

Invert (5.4.14) and multiply with $\cos^2\alpha_1$, we get

$$\frac{\cos\alpha_1}{\cos\alpha} > \frac{2e\cos^2\alpha_1}{(e^2-2)^2},$$

where using (5.4.11) in above inequality gives

$$\frac{\cos\alpha_1}{\cos\alpha} > \frac{e}{(e^2-2)^2}. \tag{5.4.15}$$

Finally by using simplified inequalities for $\tan 2\alpha$ and $\frac{\cos\alpha_1}{\cos\alpha}$ in (5.4.2), we get

$$(\tan 2\alpha)^2 \frac{\cos\alpha_1}{\cos\alpha} < (\frac{2\sqrt{e^2-1}}{e^2-2})^2 \frac{e}{(e^2-2)^2},$$

$$e < \frac{4e(\sqrt{e^2-1})^2}{(e^2-2)^4},$$

$$1 < \frac{4(e^2-1)}{(e^2-2)^4}. \tag{5.4.16}$$

which implies $e \leq 1.95$, giving an upper bound for e.

Hence

$$\sqrt{2} < e \leq 1.95,$$

is a necessary condition for a material for the existence of mode conversion.

Chapter 6

Conclusion

The very well-known Rayleigh-Lamb frequency relation for an isotropic plate is studied and the intersection between symmetric and antisymmetric Lamb modes is discussed. A MATLAB code is generated to sketch the Lamb mode dispersion curves related with each expression and there intersections are also graphically represented.

The intersection points for symmetric and anti symmetric Lamb modes are determined in k-c plane and they agree very well with the intersection points studied in k-Ω plane.

We have likewise analyzed that there is a region where slope of the intersected Lamb mode curves turns out to be about zero giving rise to the plateau region. The plateau region for different materials is graphically represented.

The reflection of SV-waves in a half space is mathematically studied. An analytical expression in e is derived for mode conversion to take place by using the solution set calculated for reflected SV-waves and it gives the following bound for mode conversion, $\sqrt{2} < e \leq 1.95$.

Bibliography

[1] J. Rayleigh, *The Theory of Sound*, Dover, New York, (1945).

[2] H. Lamb, *"On waves in an elastic plate,"* Proceedings of the Royal Society of London Series, **93**, 114 – 128, (1917).

[3] R. Mindlin, *"Mathematical theory of vibrations of elastic plates,"* Proceedings of the 11th Annual Symposium on Frequency Control, U.S. Army Signal Engineering Laboratories, Fort Monmouth, New Jersey, 1 – 40, (1957).

[4] D. Worlton, *"Experimental Confirmation of Lamb Waves at Megacycle Frequencies,"* Journal of Applied Physics, **32**, 967 – 971, (1961).

[5] A. Freedman, *"The variation, with the Poisson ratio, of Lamb modes in a free plate,"* Journal of Sound and Vibration, **137**, 209 – 230, (1990).

[6] A. G. Every, *"Intersections of the Lamb mode dispersion curves of free isotropic plates,"* Acoustical society of America, **139**, (2016).

[7] E. Glushkov, N. Glushkova, and C. Zhang, *"Surface and pseudo-surface acoustic waves piezoelectrically excited in diamond-based structures,"* Journal of Applied Physics, **112**, 064911 (2012).

[8] M. Benetti, D. Cannata, F. Di. Pietrantonio, V. I. Fedosov, and E. Verona, *"Gigahertz-range electro-acoustic devices based on pseudo-surface-acoustic waves in AIN/diamond/Si structures,"* Journal of Applied Physics, **87**, 033504 (2005).

[9] J. D. Achenbach, *"Waves Propagation in Elastic Solids,"* North Holland, New York, (1980).

[10] F. Ahmad, *"Shape of dispersion curves in the Rayleigh-Lamb spectrum,"* Arch. Mech., **56**, 157 − 165, (2004).

[11] F. Ahmad, *"A simple formula for the Lamb modes in a plate,"* J. Acoust. Soc. Am., **111**, 1974 − 75, (2002).

[12] F. Ahmad, *"A simple formula for the longitudinal modes in a cylinder,"* J. Acoust. Soc. Am., **115**, 475 − 477, (2004).